Collision properties of nonlinear waves in the modified Gardner equation

W Manganye

orcid.org 0000-0002-0345-3609

Dissertation accepted in fulfilment of the requirements for the degree Master of Science in Applied Mathematics at the North-West University

Supervisor: Dr RY M'pika Massoukou

Co-supervisor: Dr LD Moleleki

Graduation: July 2024

COLLISION PROPERTIES OF NONLINEAR WAVES IN THE MODIFIED GARDNER EQUATION

by

Wendy Manganye (29537223)

Dissertation submitted in fulfillment of the requirements for the degree of Masters in Applied Mathematics in the School of Mathematical and Statistical Sciences in the Faculty of Natural and Agricultural Sciences at North-West University, Mafikeng Campus

October 2023

Supervisor: Dr RY M'pika Massoukou

Co-supervisor: Dr LD Moleleki

Contents

Acknowledgement

First and foremost, I want to express my gratitude to Almighty God for providing me with the strength during the course of this work. It gives me great pleasure to express my heartfelt gratitude and thankful acknowledgement to my esteemed supervisor Dr Massoukou and co-supervisor Dr Moleleki. Their enthusiasm for Applied Mathematics has been an ongoing source of inspiration for me. I would like to take this opportunity to express my gratitude to Dr Olivier for guidance with numerical work. My sincere gratitude and special thanks go out to my family and friends for their love, inspiration and supportive assistance. Moreover, I would like to thank the North-West University and the department of Mathematical Sciences for giving me this opportunity to study. Finally, I am appreciative of SANSA bursary for financial assistance.

Abstract

Small-amplitude ion-acoustic waves near supercritical plasma compositions are described by the modified Gardner (mG) equation. In this dissertation, we analyze solutions of the mG equation and simulate collision of soliton-type solutions. The presence of nonlinear waves is strongly influenced by the coefficients of the mG equation.

First of all, we conduct an analytical analysis of the parameter space of the mG equation in order to identify coefficients where interesting nonlinear solutions such as kinks, the coexistence of positive and negative solitons, and supersolitons occur. We begin by introducing a moving frame analysis, which reduces the mG equation to a second order ordinary differential equation (ODE). This is evaluated using roots of a related cubic polynomial. Using a cubic polynomial analysis, we can determine the plasma compositional requirements for nonlinear waves, and the solutions are graphically represented. The existence of nonlinear waves and supercritical compositions are thus characterised by our research.

In addition, we use numerical simulation to study the collision properties between different nonlinear waves and with regular solitons. To construct the initial conditions on sufficiently large spatial intervals, we determine the tails through an asymptotic analysis. This is accomplished by expanding the Sagdeev pseudopotential function using a Taylor series expansion. After constructing the initial condition, a MATLAB code is developed to numerically integrate the mG equation. In this code, the spatial component is discretized using the finite difference method, and the time component is integrated using the fourth-order Runge-Kutta method. We performed numerical simulations of overtaking collisions between regular solitons and other nonlinear structures. These results may be useful in deepening the understanding of nonlinear waves in space plasmas.

Keywords: Modified Gardner equation; numerical simulations; supersolitons.

Chapter 1

Introduction

1.1 Historical background

We start this section with a brief review of the historical developments and findings that gave rise to the soliton idea.

1.1.1 Solitary wave and soliton

A solitary wave is a localized wave that propagates along one space direction only, with undeformed shape. A soliton is a very stable solitary wave, the exact solution of a wave equation whose shape and speed are not altered by a collision with other solitary waves. A soliton is a unique wave that can move without dispersion, resulting in an uncommon nonlinear phenomenon. Solitons can be observed in both continuous and discrete systems [1].

1.1.2 Historical background of solitons

A Scottish engineer named John Scott Russell made the first experimental observation of solitary waves in August 1834. He first noticed this phenomenon while inspecting the Union Canal on Edinburgh. He was watching a boat being pulled by two horses as it traveled at the canal at Edinburgh.

Immediately after the boat came to a stop, the water in the area began to move. Russell is an appropriate person to quote here: "It accumulated round the prow of the vessel in a state of violent agitation, then suddenly leaving it behind, rolled forward with great velocity, assuming the form of a large solitary elevation, a round, smooth and well-defined heap of water, which continued its course along the channel apparently without change of form or diminution of speed" [2]. He pursued it on horseback, overtaking it while it was still moving at about eight or nine miles per hour, retaining its original dimensions of thirty feet long and a foot to a foot and a half in height. After a one to two miles chase, its height gradually decreased, and Russel lost it in the canal's windings. That unique and pleasant phenomenon, which he has named the "Wave of Translation", was Russell's first chance encounter. Russell actually came up with the term "solitary wave". Russell conducted laboratory experiments in order to further investigate this new phenomenon by dropping weights in one end of a tank, thus creating solitary waves. He discovered that one or several solitary waves can form depending on how much water is displaced and that the wave's velocity is dependent on the depth of the water. The velocity was found to increase with greater depth.

The first theoretical studies on the solitary wave were conducted by Joseph Boussinesq [3], who obtained an equation for the shape of a solitary wave as well as the same velocity of propagation as Russell deduced from his experiments. Lord Rayleigh rediscovered it in 1876 using a different method. Rayleigh [4] studied the solitary wave theoretically and determined the shape of the solitary wave. He published a paper in 1876 to support the main findings of Russell's experiments with his mathematical theory. In 1891, McCowan [5] attempted to improve Rayleigh's theory and obtained an estimate of the wave's limiting height.

In 1895, Dutchmen Korteweg and de Vries invented a mathematical equation to explain the phenomenon observed by Russell. They derived a model equation which describes the unidirectional propagation of long waves in water of relatively shallow depth and the equation is known as the Korteweg-deVries (KdV) equation. Korteweg and de Vries showed that periodic solutions (cnoidal wave) can be found in closed form and found out that a localized solution is also found in the limit of infinite wavelength or spatial period of cnoidal wave [6], which corresponds to Russell's discovery of solitary waves. The KdV equation is intimately related to systems in which weak nonlinearity and weak dispersion compete [7]. The KdV equation offers solutions that, despite being nonlinear and dispersive, escape the negative consequences of dispersion and nonlinear distortion and always keep their distinct, localized shapes [8]. Due to the importance of the KdV equation in a variety of scientific situations, including plasma physics, water waves, and many others, it has received a lot of attention.

Enrico Fermi, John Pasta and Stan Ulam (FPU) were examining the heat conductivity of solids which initially appeared to have nothing to do with solitary waves. This was based on masses that can move only in one dimension that are coupled by nonlinear springs. The springs' strictly linear system ensures that any energy applied to a single "normal" mode always stays in that mode. In 1955, Fermi et al. [9] tried to verify the assumption by computer simulations on a one-dimensional lattice by examining the dynamic behaviour of a chain with nonlinear interactions between atoms. They initially expected that the initial energy would eventually be distributed equally among the lattice's simulated degrees of freedom. To their surprise, the system did not approach energy equipartition which indicates that the initial energy injected was not distributed among the lattice's degrees of freedom, but rather almost exclusively returned to the initial excited mode. The unexpected results obtained by FPU lead to further study of nonlinear systems.

The problem investigated in [9] was then examined by Ford [10] and Jackson [11]. It was confirmed that nonlinear terms did not guarantee the approach of the system to thermal equilibrium.

As a result of this, Zabusky and Kruskal approximated the nonlinear spring-mass system by the KdV equation in an effort to find an explanation for this FPU progression.

They used a continuum approximation to study the KdV equation because they discovered that the phenomenon was caused by only the lowest-order, long-wavelength discrete lattice modes. They found by numerical simulation that the robust pulse-like waves (solitary wave) can propagate in a system modelled by such an equation. Numerical solutions of the KdV equation used to model the continuum approximation of a nonlinear atomic lattice with periodic boundary conditions showed that these solitons collide at the same time but preserve their individual shapes and velocities with only small change in their phases. As a result, the authors invented the term soliton as a special case of a solitary wave.

In 1962, Perring and Skyrme [12] published numerical results demonstrating perfect recovery of shapes and speeds after collision, and went on to discover an exact analytical description of this phenomenon. In addition, solitons form due to a dynamic balance between dispersion and nonlinear effects in nonlinear evolution models [6].

This inspired interest in studying solitons mathematically. Gardner, Green, Kruskal, and Miura made an enormous breakthrough and in 1967, they [13] discovered an inverse scattering transform, which allowed them to solve the KdV equation analytically. This technique represented a significant advance in the mathematical theory of partial differential equations because it enabled the calculation of closed-form solutions to nonlinear equations.

1.1.3 Solitons in plasma physics

An important topic of nonlinear plasma physics is electrostatic solitary waves in plasmas. Electrostatic solitary waves have been seen in the magnetosphere of the earth [14]. Washimi and Taniuti [15] introduced reductive perturbation analysis into plasma physics through the introduction of a perturbation expansion approach that includes so-called stretched coordinates. They demonstrated that small-amplitude ion acoustic waves in a weakly nonlinear dispersive plasma could be described by the KdV equation [16]. Taniuti and Wei [17] developed a general theory for deriving the KdV equation. In the study of nonlinear wave propagation, reductive perturbation is an outstanding and efficient method of deriving relevant models. However, the method is limited to weakly nonlinear waves despite having the benefits of flexibility and numerical procedures in exploring a wide range of models.

Sagdeev [18] theoretically investigated nonlinear solitary waves in various plasma models using pseudopotential analysis. Theoretical studies often rely on Sagdeev's pseudopotential analysis. Its advantage is that it is not limited to solitary waves of small amplitudes, but allows for large but bounded solutions, given the model's various constraints.

According to Kadomtsev and Karpman [19], the development of solitary waves is caused by a precise balance between nonlinearity and dispersion. Nishikawa and Kaw [20] were the first to consider the propagation of ion acoustic KdV solitons in an inhomogeneous plasma. KdV solitons show elastic interaction properties, surviving overtaking of slower by faster solitons almost unchanged, and having characteristic relationships between amplitude, width, and propagation speed [21].

In 2012, Dubinov and Kolotkov [22] were the first to describe supersolitons in a plasma with five different species using Sagdeev pseudopotential method. Supersolitons are similar to regular solitons in the sense that they propagate without changing shape. However, where regular solitons have two inflection points, supersolitons have six inflection points. This leads to the formation of so-called "wiggles in the tails" of the corresponding electric field signatures. They located the origin of the deformations that are distinctive to supersolitons using an equilibrium point in the phase diagram [22]. Following this article, several authors reported the discovery of supersolitons in various plasma systems using the Sagdeev pseudopotential method. Das et al. [23] found supersolitons in an unmagnetized nonthermal plasma consisting of negatively charged dust grains, adiabatic positive ions and nonthermal electrons. Verheest, Hellberg, and Kourakis [24] demonstrated that the minimal number of species to support supersolitons is three in a plasma composed of cold positive and cold negative ion species and Cairns-distributed electrons. They demonstrated that double layers are not always formed as the lower limit of supersolitons. The existence of double layers was regarded to be the lower limit [25]. Supersolitons, however, can still form even in the absence of a double layer [26]. They also revealed the existence of ion-acoustic supersolitons in many three-species plasma models, each with a different plasma species composition [27], [28]. Maharaj et al. [29], Hellberg et al. [25], and Verheest [30] reported supersolitons on dust-acoustic time scales. Singh and Lakhina [31], Paul and Bandyopadhyay [32], and Olivier et al. [33] observed supersolitons in ion-acoustic time scales.

Olivier et al. [34] reported a supercritical plasma composition for a plasma consisting of cold ions and two Boltzmann electron species. They derived a modified KdV equation with a fourth-order nonlinearity and showed that plasma composition support $sech-$type solitons. The higher order KdV equation was shown to be non-integrable meaning that these solitons do not have the elastic collision properties of the regular KdV and the modified KdV (mKdV) equations.

It was previously proposed that reductive perturbation analysis could not be used for identifying supersolitons [35]. However, there was no report available at the time about supercritical plasma compositions [36]. Olivier et al. [37] recently discovered the necessary conditions for small-amplitude supersolitons to occur in a plasma consisting of cold ions and two-temperature Boltzmann electrons using reductive pertubation. They studied collision properties of overtaking supersolitons with small amplitudes and they applied reductive perturbation analysis to study small-amplitude supersolitons in a plasma. This analysis led to a generalized KdV equation which is referred to as the modified Gardner (mG) equation. Their simulations showed that the collision between solitons and supersolitons destroys the supersoliton structure to form a regular soliton. It is different from elastic collisions of regular solitons and therefore the collision is inelastic. It has been demonstrated that small-amplitude supersolitons and supercritical plasma compositions are closely related.

1.2 Motivation

The existence of supersolitons is a relatively new phenomenon in solitary wave theory of plasma physics that was first reported by Dubinov and Kolotkov [22], [38], [39]. Since then, a large number of plasma fluid models were shown to support supersolitons, including [24], [27], [28], [29], [33] .

In [37], Olivier et al. showed that these structures can be described by a generalized Korteweg-de Vries (KdV) type of equation, referred to as the modified Gardner (mG) equation. The fact that only two conservations laws were found for the mG equation, along with the fact that it fails the Painlevé test, which predicts whether an equation is likely to be integrable, shows that the equation is nonintegrable. This was also reinforced by numerical simulations of collisions between solitons and supersolitons, showing that the inelastic collision reduces the supersoliton to a regular soliton.

The study of the mG equation in [37] was limited to coefficients that support supersolitons. In this study, we relax this constraint in order to study all possible solutions of the mG equation. These solutions will be obtained by a moving frame analysis, also known as a travelling wave analysis, which allows to reduce the modified Gardner equation to an ordinary differential equation. Besides regular solitons, we also report algebraic solitons and kink solutions. The first aim of this thesis is to characterize all solitary wave solutions of the mG equation, and to determine their dependence on the coefficients of the mG equation. We will then use numerical simulation in order to study the collision properties of some of the more exotic structures with regular solitons. This study will provide deeper insight into the electrostatic dynamics of plasmas near supercritical compositions and the role of higher order nonlinear effects on soliton propagation and interaction properties.

1.3 Outline of the dissertation

This dissertation main goal is to investigate a wide range of solutions of the mG equation. The dissertation is organized as follows. The background of the study was covered in Chapter 1, including a brief introduction with definitions. We reviewed some work on solitons and the collision characteristics of nonlinear waves. The purpose of this introductory chapter is to provide readers with an introduction to the basic ideas of solitons in plasma physics. We give a review of cubic polynomials in Chapter 2, because they are crucial to solving the mG equation. The mG equation's parameter space is analytically analyzed in Chapter 3 to identify areas where irregular nonlinear solutions, such as double layers, the coexistence of positive and negative solitons, and supersolitons, occur. A numerical algorithm for solving the mG equation is described in Chapter 4 that uses the fourth-order Runge-Kutta method to integrate with respect to time and the finite difference method to discretize the spatial derivatives. The collision properties of double layers overtaking positive and negative solitons and solitons overtaking solitons are numerically simulated in Chapter 5, using the modified Gardner equation. Finally, Chapter 6 summarizes the thesis' main conclusions.

Chapter 2

Review of cubic polynomial

2.1 Introduction

Cubic polynomials play an essential role in finding the solutions of the mG equation.

2.2 Descartes' rule of signs

Descartes' rule of signs is a mathematical principle utilized in algebra to ascertain the highest possible count of real roots within a polynomial equation featuring one variable. This process analyses polynomials to investigate their roots and differentiate between identifying their roots and discern positive and negative roots [40]. Polynomials can be factorized in terms of its roots, potentially yielding multiple real roots. However, it is important to acknowledge the existence of roots that may be negative-valued. This rule operates based on tracking how often the signs of the coefficients change when the terms are systematically arranged. By employing this technique, one can deduce the signs of the coefficients necessary for determining the number of both positive and negative real roots [40]. For example, a cubic polynomial

$$P(x) = x^3 - 8x^2 - x + 8, \tag{2.1}$$

changes signs twice, so it can only have at most two positive real solutions. On the other hand

$$P(-x) = (-x)^3 - 8(-x)^2 - (-x) + 8, \tag{2.2}$$

that is,

$$P(-x) = -x^3 - 8x^2 + x + 8, \tag{2.3}$$

changes sign twice, so that it could have at most two negative roots. Consider a cubic polynomial defined in (2.1).

A cubic polynomial (2.1), have two positive roots, $x = 1$ and $x = 8$ and a negative root $x = -1$. On the other hand

$$P(-x) = -x^3 - 8x^2 + x + 8, \tag{2.4}$$

have one positive root $x = 1$ and two negative roots $x = -8$ and $x = 1$.

2.3 Roots of cubic polynomial

Consider a cubic polynomial written in the form:

$$z^3 + a_2 z^2 + a_1 z + a_0 = 0, \tag{2.5}$$

where a_2 , a_1, and a_0 are real coefficients. The discriminant can be used to determine the nature of a cubic's roots without formally determining them. The nature of the roots of a cubic polynomial is adapted here from Abramowitz and Stegun [41]. If the coefficients of a cubic polynomial are real numbers and its discriminant $\Delta = 18ABCD - 4B^3D + B^2C^2 - 4AC^3 - 27A^2D^2$ is not zero, there are two possibilities:

$$\Delta > 0 \quad \& \quad \Delta < 0.$$

If $\Delta > 0$, a cubic polynomial has three distinct real roots. As an example, consider Figure 2.1, where we show a cubic polynomial graph with three distinct real roots.

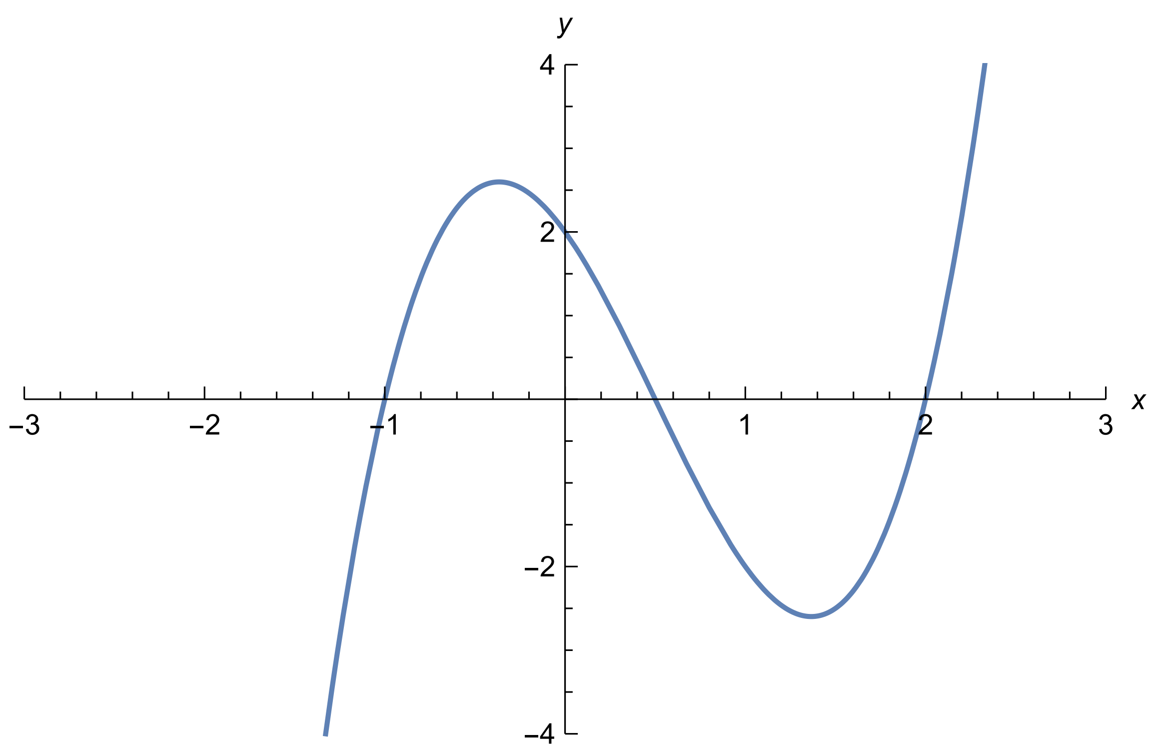

Figure 2.1: $\Delta > 0$ in this case

If $\Delta < 0$, the equation has one real root and two complex conjugate roots. Consider the Figure 2.2, which shows a cubic polynomial graph with one real root and two complex conjugates.

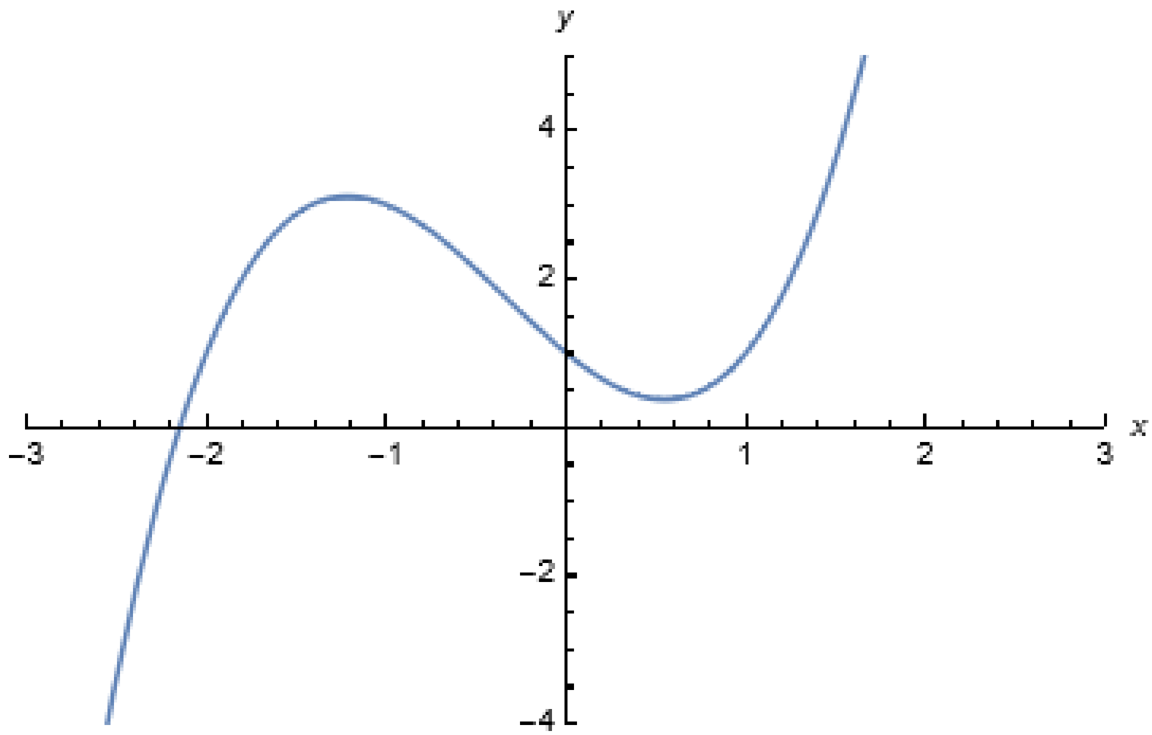

Figure 2.2: $\Delta < 0$ in this case

If a cubic polynomial's discriminant $\Delta = 0$, a cubic polynomial has a root of multiplicity greater than one. If its coefficients are also real, then all of its roots are real. If the discriminant of a cubic polynomial $z^3 + a_2z^2 + a_1z + a_0$ is zero, a cubic polynomial has either a triple root or a cubic polynomial has a double root and a simple root. Consider Figures 2.3 and 2.4, which show a cubic polynomial graph with triple root as well as a cubic polynomial graph with a double root.

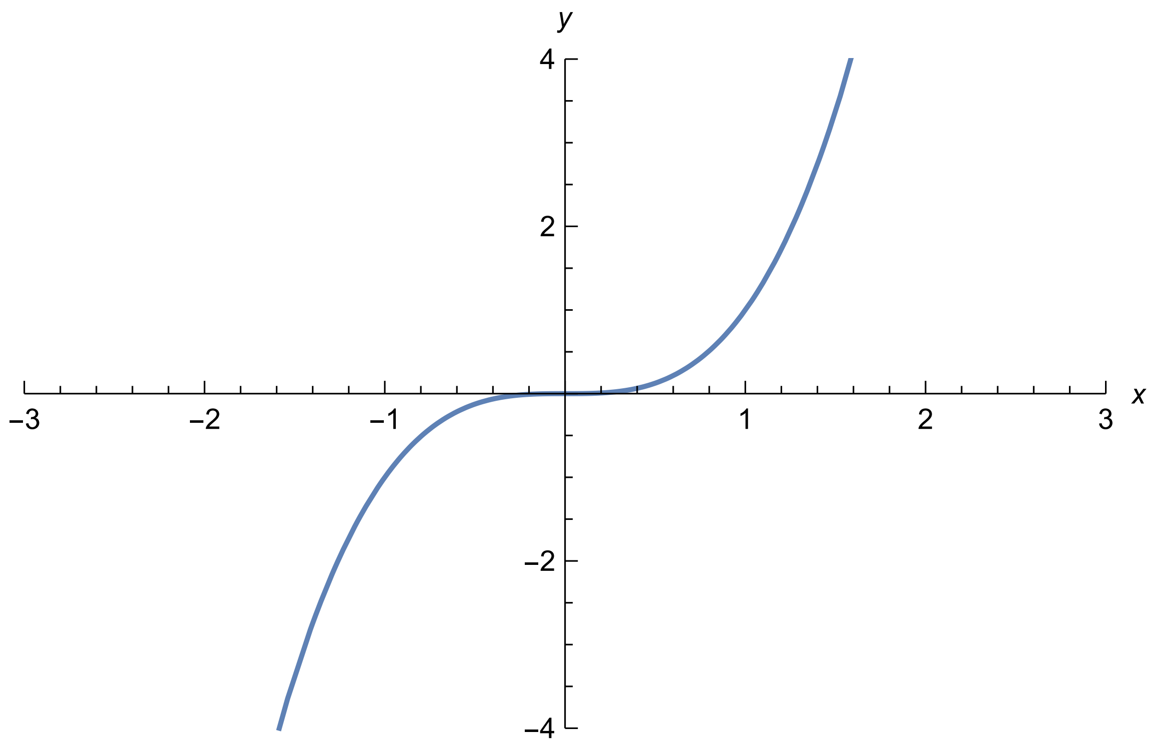

Figure 2.3: $\Delta = 0$ in this case

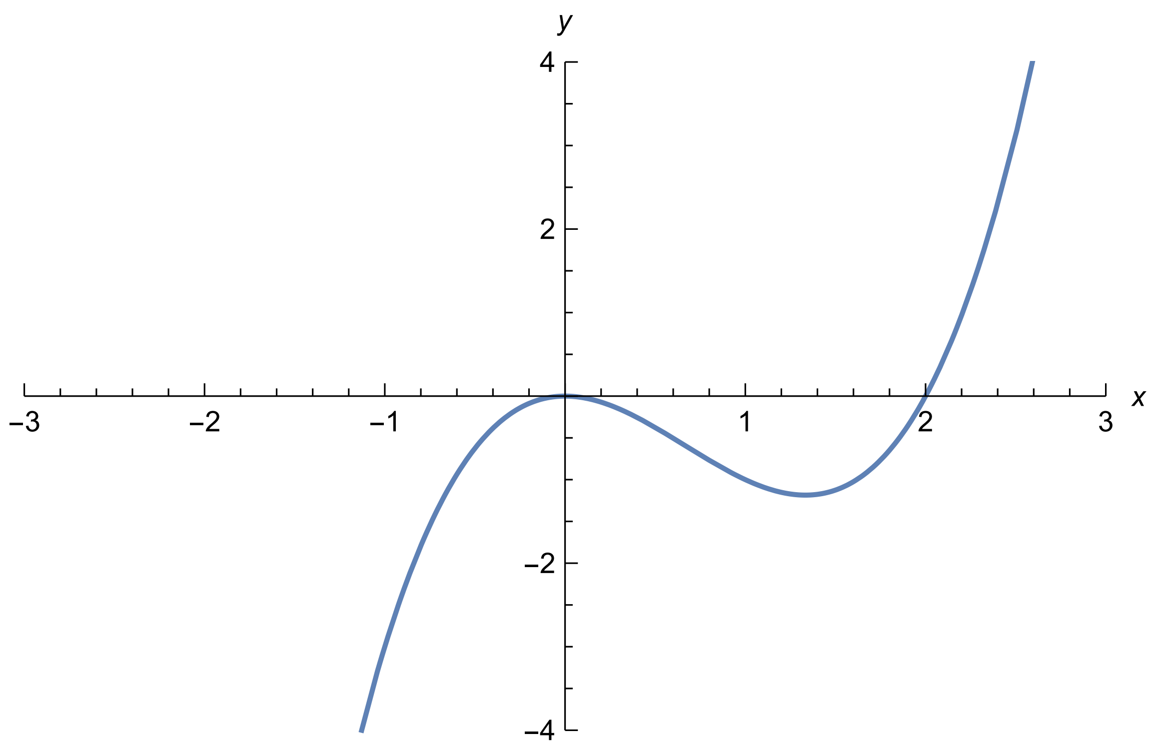

Figure 2.4: $\Delta = 0$ in this case

To examine the roots of the cubic polynomial, we study the roots of a cubic polynomial. The solutions presented below are drawn from Abramowitz and Stegun [41]. Let (2.5) be a cubic polynomial.The change of variable

$$z = t - \frac{a_2}{3}, \tag{2.6}$$

gives a cubic (in t) that has no term in t^2. After dividing by a one obtains depressed cubic equation

$$t^3 + pt + q = 0, \tag{2.7}$$

with

$$t = z + \frac{a_2}{3}, \tag{2.8}$$

$$p = \frac{3a_1 - a_2^2}{3}, \tag{2.9}$$

$$q = \frac{2a_2^3 - 9a_1a_2 + 27a_0}{27}. \tag{2.10}$$

The roots of the original equation, z_1, z_2, z_3, are connected t_1, t_2, t_3 of the depressed equation by the relations

$$z_i = t_i - \frac{a_2}{3}, \tag{2.11}$$

for $i = 1, 2, 3$.

We consider the hyperbolic solution for one real root because a supersoliton has one real root. The real root will be used later as follows

$$t_0 = -2\frac{|q|}{q}\sqrt{\frac{-p}{3}}\cosh\left[\frac{1}{3}\cosh^{-1}\left(\frac{-3|q|}{2p}\sqrt{\frac{-3}{p}}\right)\right], \tag{2.12}$$

if $4p^3 + 27q^2 > 0$ and $p < 0$, and

$$t_0 = -2\sqrt{\frac{p}{3}}\sinh\left[\frac{1}{3}\sinh^{-1}\left(\frac{3|q|}{2p}\sqrt{\frac{-3}{p}}\right)\right], \tag{2.13}$$

if $p > 0$.

Consider a cubic polynomial defined in (2.5)

The discriminant of a cubic polynomial P(ϕ) is given by Δ_3, is given as follows

$$\Delta_3 = 18ABCD - 4B^3D + B^2C^2 - 4AC^3 - 27A^2D^2. \tag{2.14}$$

For $B^2 \neq 3AC$, $\Delta_3 = 0$ has a double root given by

$$\phi_2 = \phi_3 = \frac{9AD - BC}{2(B^2 - 3AC)} = \frac{9a_0 - a_1a_2}{2(a_2^2 - 3a_1)} \tag{2.15}$$

For $B^2 = 3AC$, $\Delta_3 = 0$ has a triple root given by

$$\phi_1 = \phi_2 = \phi_3 = -\frac{B}{3A} = -\frac{a_2}{3}. \tag{2.16}$$

Chapter 3

Solutions of the modified Gardner equation

3.1 Introduction

In the previous chapter, we discussed the roots of a related cubic polynomial as they play an important role in finding regions where nonlinear waves of the mG equation occur. In this chapter, we derive the mG equation and look at the solutions of the mG equation such as positive and negative algebraic solitons, kink, and supersoliton solutions. We start by introducing a moving frame analysis that reduces the problem to a second order ODE and we will look at how cubic polynomials are important in determining the regions where nonlinear waves of mG equation occur.

3.2 General form of the modified Gardner equation

Given the mG equation of the form

$$\frac{\partial \phi}{\partial t} + \frac{1}{2}\frac{\partial^3 \phi}{\partial x^3} + A\phi\frac{\partial \phi}{\partial x} + B\phi^2\frac{\partial \phi}{\partial x} + C\phi^3\frac{\partial \phi}{\partial x} = 0. \tag{3.1}$$

Setting

$$T = \alpha t, \quad X = \beta x, \quad and \quad \phi = \gamma \Phi, \tag{3.2}$$

in order to determine the values of α, β and γ so that we can express the mG equation in normalized form. The following equation for the time derivative is obtained

$$\frac{\partial}{\partial t} = \alpha \frac{\partial}{\partial T} \tag{3.3}$$

and the following equations for the space derivatives

$$\frac{\partial}{\partial x} = \beta \frac{\partial}{\partial X}, \tag{3.4}$$

$$\frac{\partial^3}{\partial x^3} = \beta^3 \frac{\partial^3}{\partial X^3}. \tag{3.5}$$

Therefore, ϕ_t, ϕ_{xxx}, $\phi\phi_x$, $\phi^2\phi_x$, $\phi^3\phi_x$ can be expressed respectively, as follows

$$\phi_t = \frac{\partial \phi}{\partial t} = \frac{\alpha}{\gamma} \Phi_T \tag{3.6}$$

$$\phi_x = \frac{\partial \phi}{\partial X} \tag{3.7}$$

$$\phi_{xxx} = \frac{\partial^3 \phi}{\partial x^3} = \frac{\beta^3}{\gamma} \Phi_{XXX} \tag{3.8}$$

$$\phi\phi_x = \frac{\beta}{\gamma^2} \Phi\Phi_X \tag{3.9}$$

$$\phi^2\phi_x = \frac{\beta}{\gamma^3} \Phi^2\Phi_X \tag{3.10}$$

$$\phi^3\phi_x = \frac{\beta}{\gamma^4} \Phi^3\Phi_X. \tag{3.11}$$

By substituting the expressions (3.6), (3.8), (3.9), (3.10) and (3.11) into (3.1), one obtains the following equation

$$\Phi_T + \frac{\beta^3}{2\alpha}\Phi_{XXX} + \frac{A\beta}{\alpha\gamma}\Phi\Phi_X + \frac{B\beta}{\alpha\gamma^2}\Phi^2\Phi_X + \frac{C\beta}{\alpha\gamma^3}\Phi^3\Phi_X = 0. \tag{3.12}$$

The first step in the normalization process is to set the coefficients of Φ_{XXX} to $\frac{1}{2}$. This value is chosen for consistency with the standard form of the KdV equation in plasma physics. It follows that

$$\alpha = \beta^3 \tag{3.13}$$

Similarly, setting the coefficient of $\Phi^3\Phi_X$ to one gives

$$\beta^2 = \frac{C}{\gamma^3}. \tag{3.14}$$

Next, we set the coefficients of the terms $\Phi\Phi_X$ and $\Phi^2\Phi_X$ equal to a and b, respectively, so that

$$a = \frac{A}{C}\gamma^2 \tag{3.15}$$

and

$$b = \frac{B}{C}\gamma. \tag{3.16}$$

To further simplify the coefficients a and b, we represent the parametric vector $[b, a]^T$ in polar coordinates. This yields

$$\begin{bmatrix} b \\ a \end{bmatrix} = \begin{bmatrix} r\cos\theta \\ r\sin\theta \end{bmatrix},$$

where

$$r = \sqrt{a^2 + b^2} \tag{3.17}$$

and

$$\tan\theta = \frac{a}{b} = \frac{A}{B}\gamma. \tag{3.18}$$

In addition, we can set $r = 1$ by setting $a^2 + b^2 = 1$, so that

$$A^2\gamma^4 + B^2\gamma^2 - C^2 = 0, \tag{3.19}$$

so that

$$\gamma^2 = \frac{-B^2 + \sqrt{B^4 + 4A^2C^2}}{2A^2}. \tag{3.20}$$

It then follows that

$$a = \sin\theta, b = \cos\theta$$

and we arrive at the normalized form of the mG equation

$$\frac{\partial \Phi}{\partial T} + \frac{1}{2}\frac{\partial^3 \Phi}{\partial X^3} + a\Phi\frac{\partial \Phi}{\partial X} + b\Phi^2\frac{\partial \Phi}{\partial X} + \Phi^3\frac{\partial \Phi}{\partial X} = 0. \tag{3.21}$$

Note that (3.1) can always be normalized into this form unless $C = 0$ or $A = B = 0$.

3.3 Sagdeev potential method

Consider the normalized mG equation (3.21) introduced in the previous section, where the following assumptions are made:

$$a = \sin\theta, \;\; b = \cos\theta, \;\; and \;\; c = 1.$$

Equation (3.21) has been reported in [37], where the study was limited to the values of the coefficients that yield supersolitons. We are interested in solitons, kink and supersolitons. We impose the following boundary condition:

$$\phi \to 0 \quad \text{as} \quad x \to +\infty. \tag{3.22}$$

In order to obtain solutions to (3.1), we introduce a moving frame

$$\xi = x - mt, \tag{3.23}$$

where m denotes the speed. The derivative of ϕ with respect of t and x, respectively, can then be expressed in terms of ξ as follows:

$$\frac{\partial \phi}{\partial t} = -m\frac{d\phi}{d\xi}, \tag{3.24}$$

$$\frac{\partial \phi}{\partial x} = \frac{d\phi}{d\xi}, \tag{3.25}$$

$$\frac{\partial^3 \phi}{\partial x^3} = \frac{d^3\phi}{d\xi^3}. \tag{3.26}$$

By substituting the expressions (3.24), (3.25) and (3.26) into (3.1) one obtains the ordinary differential equation

$$-m\phi_\xi + \frac{1}{2}\phi_{\xi\xi\xi} + a\phi\phi_\xi + b\phi^2\phi_\xi + c\phi^3\phi_\xi = 0, \tag{3.27}$$

which is equivalent to

$$-m\phi_\xi + \frac{1}{2}\phi_{\xi\xi\xi} + \frac{1}{2}a(\phi^2)_\xi + \frac{1}{3}b(\phi^3)_\xi + \frac{1}{4}c(\phi^4)_\xi = 0. \tag{3.28}$$

Integrating (3.28) with respect to ξ gives

$$-m\phi + \frac{1}{2}\phi_{\xi\xi} + \frac{1}{2}a\phi^2 + \frac{1}{3}b\phi^3 + \frac{1}{4}c\phi^4 = 0. \tag{3.29}$$

Multiply equation (3.29) by ϕ_ξ, we obtain

$$-m\phi\phi_\xi + \frac{1}{2}\phi_{\xi\xi}\phi_\xi + \frac{1}{2}a\phi^2\phi_\xi + \frac{1}{3}b\phi^3\phi_\xi + \frac{1}{4}c\phi^4\phi_\xi = 0, \tag{3.30}$$

which is equivalent to

$$\frac{-m}{2}(\phi^2)_\xi + \frac{1}{4}(\phi_\xi^2)_\xi + \frac{a}{6}(\phi^3)_\xi + \frac{b}{12}b(\phi^4)_\xi + \frac{c}{20}(\phi^5)_\xi = 0. \tag{3.31}$$

Integrating equation (3.31) with respect to ξ then gives

$$\frac{-m}{2}\phi^2 + \frac{1}{4}\phi_\xi^2 + \frac{a}{6}\phi^3 + \frac{b}{12}b\phi^4 + \frac{c}{20}\phi^5 = 0, \tag{3.32}$$

which yields

$$\frac{1}{2}\phi_\xi^2 + \phi^2\left(\frac{c}{10}\phi^3 + \frac{b}{6}\phi^2 + \frac{a}{3}\phi - m\right) = 0. \tag{3.33}$$

The subscript ξ is used to denote the derivative $d/d\xi$. Therefore, we write equation (3.33) as energy-like integral,

$$\frac{1}{2}(\frac{d\phi}{d\xi})^2 + V(\phi, m) = 0, \tag{3.34}$$

where $V(\phi, m)$ is a function of the electrostatic potential, often known as the Sagdeev potential [18]. This function is expressed as

$$V(\phi, m) = \phi^2 \left[\frac{c}{10}\phi^3 + \frac{b}{6}\phi^2 + \frac{a}{3}\phi - m\right]. \tag{3.35}$$

Choosing $A = c/10$, $B = b/6$, $C = a/3$, and $D = -m$, (3.35) becomes

$$V(\phi) = \phi^2[A\phi^3 + B\phi^2 + C\phi + D]. \tag{3.36}$$

By substituting $a = \sin\theta$, $b = \cos\theta$, and $c = 1$, it follows that

$$A = \frac{1}{10}, \quad B = \frac{1}{6}\cos\theta \quad , \quad C = \frac{1}{3}\sin\theta \quad and \quad D = -m. \tag{3.37}$$

3.4 Conditions for existence of the kink

Another important class of nonlinear solutions are known as kink solutions. Like solitons, kinks propagate at the acoustic speed. However, solitons require a non-zero root in the Sagdeev potential, whereas kinks form a multiple root in the corresponding Sagdeev potential. In most cases, this consist of a double root (local minimum). Kink solutions was first reported by Langmuir [42], which he called "double sheath." A kink is known as a double-layer in plasma physics.

In this section, we investigate the conditions required to obtain both positive and negative kink solutions. The Sagdeev potential must have a double root, which means that the discriminant must be equal to zero. Kink solutions arise at a critical speed in the form of a nontrivial root of the Sagdeev potential that is charge neutral. The resulting double layer solutions take on ramp-like shapes in the electrostatic potential.

There are two approaches to addressing boundary conditions for developing kinks solutions. Kink speed only impacts one side of the tail. The multiplicity of the double layer root influences the tail's opposite side. The kink solution exists in two conditions:

$\phi \to \phi_r$ when $\xi \to -\infty$ and $\phi \to 0$ when $\xi \to +\infty$.

Consider Figure 3.1 where we show a positive and a negative kink solution of the modified Gardner equation.

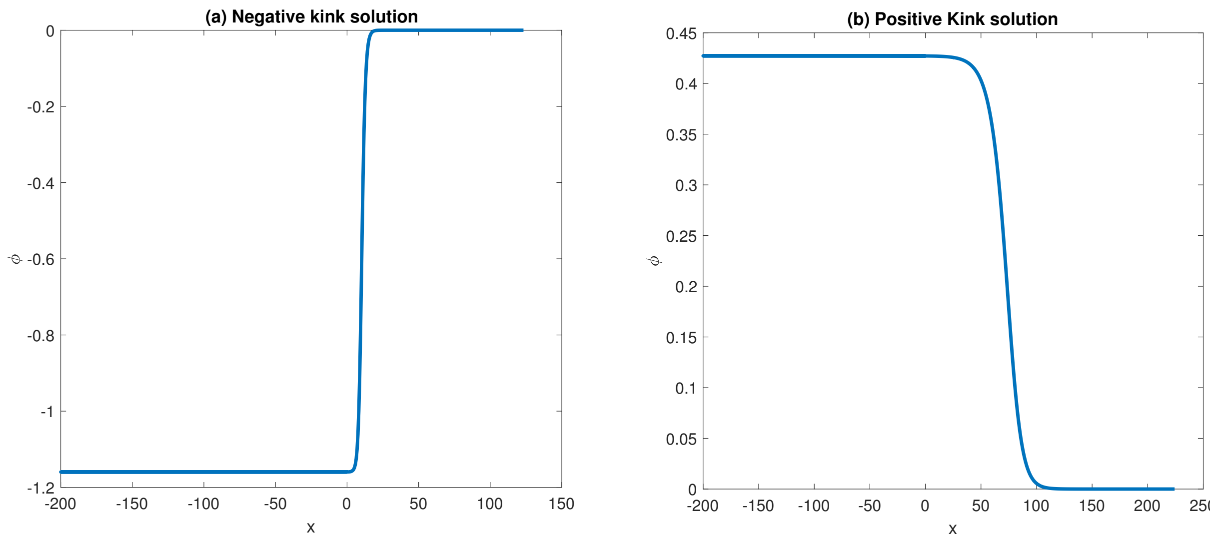

Figure 3.1: In (a) We show a negative kink solution at $\theta = -1.370796$ and in (b) we show a positive kink solution at $\theta = 2.889475$.

3.4.1 Conditions for existence of a negative kink

To obtain a negative kink, we must first locate the region where the negative kink exists in terms of θ. For an algebraic soliton, the Sagdeev potential must have two nonzero roots, and $m = 0$ indicates that the soliton is stationary. There is a kink wherever there is an algebraic soliton. In this case, we let $m = 0$ to find a region with an algebraic soliton, and once we find the regions, we know that the turning point is above the x-axis. We know that increasing m lowers the turning point until it is on the x-axis, where it forms a double root. After determining θ, we compute the negative kink speed for any θ satisfying $\Delta_2 > 0$ where Δ_2 is defined by (3.38) below.

To start off, we consider the following conditions: $m = 0$, and $\Delta_2 > 0$, where

$$\Delta_2 = B^2 - 4AC. \tag{3.38}$$

For $m = 0$, the potential function defined in (3.36), becomes

$$V(\phi) = \phi^3(A\phi^2 + B\phi + C). \tag{3.39}$$

The existence of kink solutions depends on the existence of two non-trivial roots of the potential function. Therefore, $B^2 - 4AC > 0$; that is,

$$\frac{\cos^2\theta}{36} - \frac{4}{10}\frac{\sin\theta}{3} > 0. \tag{3.40}$$

The equation (3.40) can be simplified further, yielding

$$-1 < \sin\theta < \frac{1}{5}. \tag{3.41}$$

Therefore

$$-\frac{\pi}{2} < \theta < 0.201. \tag{3.42}$$

In order to obtain our kink, the value of θ must range between $-\pi/2$ and 0.201. To calculate the kink speed for any θ values satisfying $\Delta_2 > 0$, we use the equation (3.36) to find $\Delta_3 = 0$ at $m = m_k$.

Consider the Sagdeev potential in (3.36). In terms of the roots, the factor ϕ^2 simply gives rise to a double root at the origin.

For nonzero roots, we consider a cubic polynomial

$$P(\phi) = -m + C\phi + B\phi^2 + A\phi^3. \tag{3.43}$$

The discriminant of a cubic polynomial P(ϕ) is given by Δ_3, as given in (2.14).

Substituting A, B and C, as given in (3.37), reduces Δ_3 to a quadratic polynomial in m, whose roots are given by

$$\begin{aligned} m =& \frac{50}{27}\left(\left(-\frac{\sin\theta\cos\theta}{10} + \frac{\cos^3\theta}{54}\right)\right. \\ &+ \left.\sqrt{\left(\frac{\sin\theta\cos\theta}{10} - \frac{\cos^3\theta}{54}\right)^2 - \left(\frac{-\cos^2\theta\sin^2\theta}{300} + \frac{2\sin^3\theta}{125}\right)}\right). \end{aligned} \tag{3.44}$$

The above equation was derived analytically.

After substituting A, B and C, as given in (3.37), into (2.15), we obtain

$$\phi_2 = \phi_3 = -\frac{\frac{-9}{10}m + \frac{1}{18}\sin\theta\cos\theta}{\frac{1}{18}\cos^2\theta - \frac{1}{5}\sin\theta}. \tag{3.45}$$

As an example, consider Figure 3.2 (a) where we show the Sagdeev potential at the critical speed (m) where the kink occurs at $\theta = -1.370796$ and $m = 0.267424$. It shows that the double root forms at $\phi = -1.159726$. In the Figure 3.2 (b), we show the solution of the modified Gardner equation.

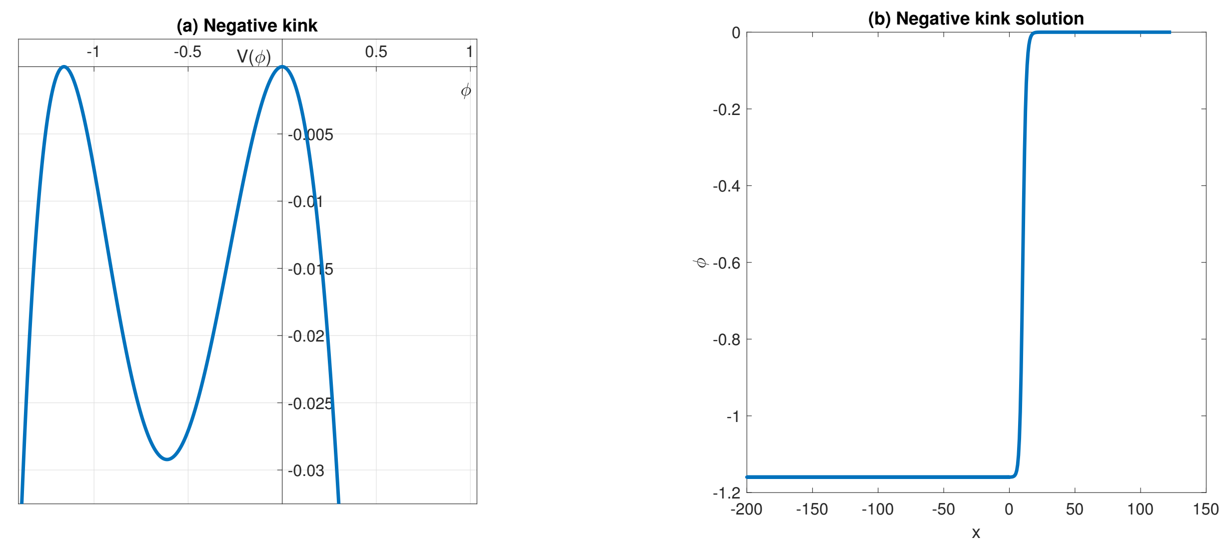

Figure 3.2: The Sagdeev potential for a negative kink is shown in (a) where the double root forms at $\phi = -1.159726$, $\theta = -1.370796$ and $m = 0.267424$. In (b) the solution of the modified Gardner is shown.

3.4.2 Conditions for existence of a positive kink

In order to obtain a positive kink, the following conditions must be met:

$a > 0$, $b < 0$ and $B^2 - 4AC \geq 0$. The positive kink requires $\Delta_3(m) = 0$ and $\Delta_3(m)$ will have real roots when $B^2 - 4AC \geq 0$.

Consider a cubic polynomial (3.43). Therefore the discriminant of a cubic polynomial is given by Δ_3 as given in (2.14), and we get

$$\frac{27m^2}{100} + \left(\frac{\sin\theta\cos\theta}{10} - \frac{\cos^3\theta}{54}\right) m + \left(\frac{2\sin^3\theta}{135} - \frac{\sin^2\theta\cos^2\theta}{324}\right). \tag{3.46}$$

The above equation was derived analytically.

Since $B^2 - 4AC \geq 0$, we obtain

$$\left(\frac{\sin\theta\cos\theta}{10} - \frac{\cos^3\theta}{54}\right)^2 - \left(\frac{-\cos^2\theta\sin^2\theta}{300} + \frac{2\sin^3\theta}{125}\right) \geq 0 \tag{3.47}$$

By solving the above equation numerically, we find that θ is as follows:

$$2.879475 < \theta < \pi. \tag{3.48}$$

As mentioned earlier that $a > 0$, $b < 0$ where $a = \sin\theta$, $b = \cos\theta$. Hence,

$$\begin{aligned} m =& \frac{50}{27}\Bigg(\left(-\frac{\sin\theta\cos\theta}{10} + \frac{\cos^3\theta}{54}\right) \\ &+ \sqrt{\left(\frac{\sin\theta\cos\theta}{10} - \frac{\cos^3\theta}{54}\right)^2 - \left(\frac{-\cos^2\theta\sin^2\theta}{300} + \frac{2\sin^3\theta}{125}\right)}\Bigg). \end{aligned} \tag{3.49}$$

As an example, consider Figure 3.3 (a), where we show the Sagdeev potential at the critical speed (m) where the kink occurs at $\theta = 2.889475$ and $m = 0.013864$. The figure shows that the double root forms at $\phi = 0.427252$ in agreement with the double root given by (2.15). In Figure 3.3 (b), we show the solution of the modified Gardner equation.

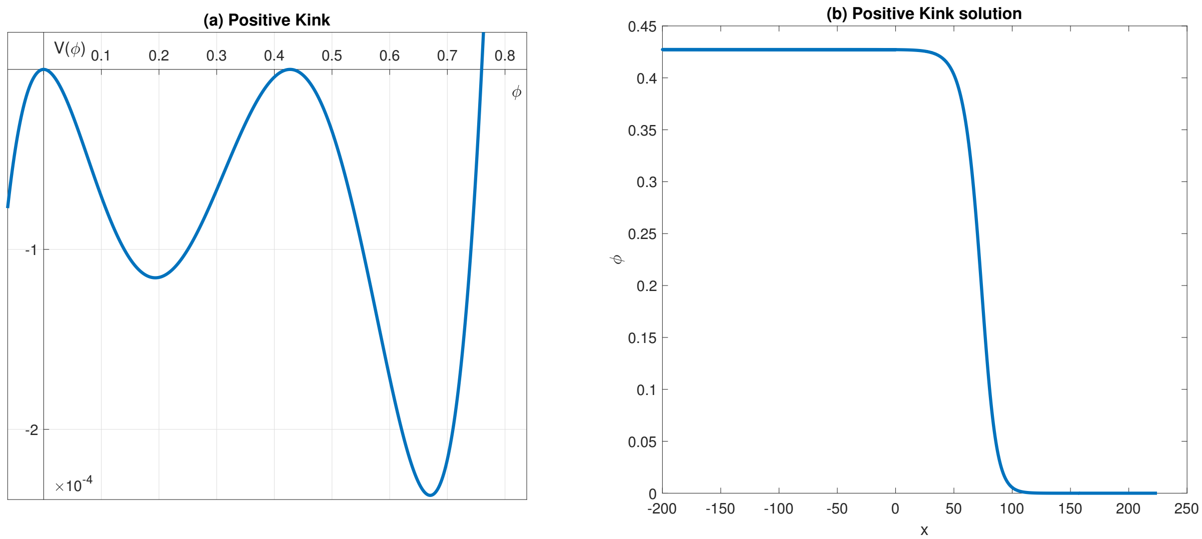

Figure 3.3: The Sagdeev potential for a positive kink is shown in (a) where the double root forms at $\phi = 0.427252$, $\theta = 2.889475$ and $m = 0.013863$. In (b) the solution of the modified Gardner is shown.

In Figure 3.4 we show the Sagdeev potential at the special case of a positive kink when a triple root forms instead of a double root. We choose $\theta = 2.879475$ where $B^2 = 3AC$ so that Sagdeev potential has a triple root. From equation (2.16) we know that the triple root forms at $\phi = 0.536580$ at speed $m = 0.015449$.

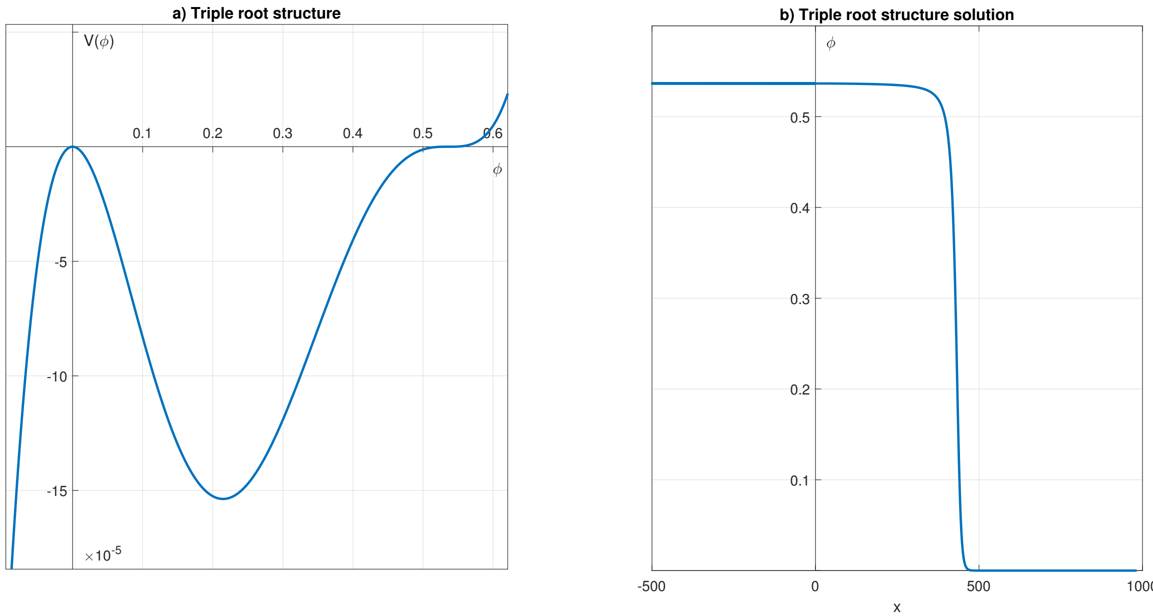

Figure 3.4: Sagdeev potential of the triple root structure that forms at $\theta = 2.879475$ and $m = 0.015449$.

3.5 Supersoliton

In this section, we will take a look at a supersoliton solution bounded by a kink, as well as one not bounded by a kink. There must be two local minimums and one local maximum, with all of them being positive. This indicates that the derivative of the Sagdeev potential must have three distinct nontrivial roots. In this case, the discriminant of the derivative must be greater than zero. If the Sagdeev potential has an additional root beyond the kink, supersolitons may arise at speeds above the critical speed. For such plasma compositions, the kink speed acts as a lower limit of supersoliton speed. Supersolitons were discovered in many studies by looking for a kink with an additional root beyond the kink amplitude. The Sagdeev potential has a root beyond the critical point. Supersolitons do not appear in all kink solutions. However, the presence of supersoliton solutions does not always indicate the presence of kink solutions. A supersoliton solution has three negative turning points of the Sagdeev potential.

It is worth noting that the Sagdeev potential $V(\phi)$ coincides with the one found in a small-amplitude study [34], using a Taylor series expansion of the Sagdeev potential. From that paper, we summarize the presence of a supersoliton:

Supersolitons can exist only if the parameters a, b, and c fulfill the following relation [34]:

$$B < 0, \quad C > 0, \quad C \leq \frac{B^2}{4A}. \tag{3.50}$$

Substituting $A = c/10$, $B = b/6$ and $C = a/3$ into the above, we obtain

$$b < 0, \quad a > 0, \quad a \leq \frac{5}{72}b^2. \tag{3.51}$$

3.5.1 Supersoliton bounded by a kink

We consider a Sagdeev potential given in (3.36). In terms of the roots, the factor ϕ^2 simply gives rise to a trivial double root at the origin. The nontrivial roots arise as roots of a cubic polynomial,

$$P(\phi) = 0, \tag{3.52}$$

where $P(\phi)$ is given in (3.43).

A cubic polynomial (3.43) has at most three real roots. To give rise to supersolitons, all three roots must be either positive or negative. One can begin by applying Descartes' rule of signs. This method allows us to determine the coefficients' signs that must be found in order to find either three positive or three negative real roots. Since $D < 0$, it follows that $C > 0$, $B < 0$, and $A > 0$. However, in order for them to be three negative roots, all of the coefficient signs must be the same. In this case we are only focusing on the positive roots. The conditions below are taken from [34] For the possibility of three positive roots, we must have

$$B < 0, A > 0, C > 0. \tag{3.53}$$

In order to obtain the root of the supersoliton, consider the depressed and the solutions stated below from equation (3.54)-(3.59) are taken from Abramowitz and

Stegun [41]

$$t^3 + pt + q = 0, \tag{3.54}$$

where

$$t = x + \frac{B}{3A}, \tag{3.55}$$

$$p = \frac{3AC - B^2}{3A^2}, \tag{3.56}$$

$$q = \frac{2B^3 - 9ABC + 27A^2D}{27A^3}. \tag{3.57}$$

Note that a supersoliton has only one real root, in this case we will use a hyperbolic solution for one real root which is as follows

$$t_0 = -2\frac{|q|}{q}\sqrt{\frac{-p}{3}}\cosh\left[\frac{1}{3}\cosh^{-1}\left(\frac{-3|q|}{2p}\sqrt{\frac{-3}{p}}\right)\right], \tag{3.58}$$

if $4p^3 + 27q^2 > 0$ and $p < 0$, and

$$t_0 = -2\sqrt{\frac{p}{3}}\sinh\left[\frac{1}{3}\sinh^{-1}\left(\frac{3|q|}{2p}\sqrt{\frac{-3}{p}}\right)\right], \tag{3.59}$$

if $p > 0$.

To calculate the minimum speed (m_{min}), we use the Sagdeev potential (3.36) to find the solutions of $\Delta_3 = 0$.

The discriminant of a cubic polynomial $P(\phi)$ is given in (2.14).

Subtituting A, B and C as given in (3.37) and simplifying (3.43), yields

$$\begin{aligned} m_{min} >& \frac{50}{27}\Bigg(\left(-\frac{\sin\theta\cos\theta}{10} + \frac{\cos^3\theta}{54}\right) \\ &+ \sqrt{\left(\frac{\sin\theta\cos\theta}{10} - \frac{\cos^3\theta}{54}\right)^2 - \left(\frac{-\cos^2\theta\sin^2\theta}{300} + \frac{2\sin^3\theta}{125}\right)}\Bigg). \end{aligned} \tag{3.60}$$

To calculate the maximum speed (m_{max}), we use the equation (3.36) to find the solution of $\Delta_3' = 0$.

The derivative of the Sagdeev potential is given by

$$V(\phi) = \phi(-2m + 3C\phi + 4B\phi^2 + 5A\phi^3). \tag{3.61}$$

For nonzero roots, we consider a cubic polynomial

$$P_2(\phi) = -2m + 3C\phi + 4B\phi^2 + 5A\phi^3. \tag{3.62}$$

The discriminant of a cubic polynomial P_2 is given by $\Delta_3 = 0$.

Subtituting A, B and C as given in (3.37), reduces to a quadratic polynomial in m,whose roots are given by

$$\begin{aligned} m_{max} <& \frac{1}{54}\left(\left(\frac{64\cos^3\theta}{27} - 12\sin\theta\cos\theta\right)\right. \\ &\left. \pm\sqrt{\left(-\frac{64\cos^3\theta}{27} + 12\sin\theta\cos\theta\right)^2 - \left(216\sin^3\theta - 48\sin^2\theta\cos^2\theta\right)}\right). \end{aligned} \tag{3.63}$$

Therefore

$$m_{min} < m < m_{max}. \tag{3.64}$$

As an example, consider Figure 3.5 (a) where we show the behaviour of the Sagdeev potential at $\theta = 2.889475$ for different values of the speed (m). We show that Sagdeev potential as it gives rise to a supersoliton with a kink. The grey curve shows the Sagdeev potential at a critical speed where a kink occurs at $m_{min} = 0.013864$. The blue curve shows a supersoliton that occurs at $m = 0.5*(m_{min}+m_{max})$. The purple curve shows the Sagdeev potential that arises below a supersoliton at $m_{max} = 0.015122$. The red curve shows the Sagdeev potential that arises below m at $m = 0.0155$. In (b), we show the solution of the modified Gardner equation. The modified Gardner equation gives rise to a supersoliton at $\theta = 2.889475$ and $m = 0.5 * (m_{min} + m_{max})$.

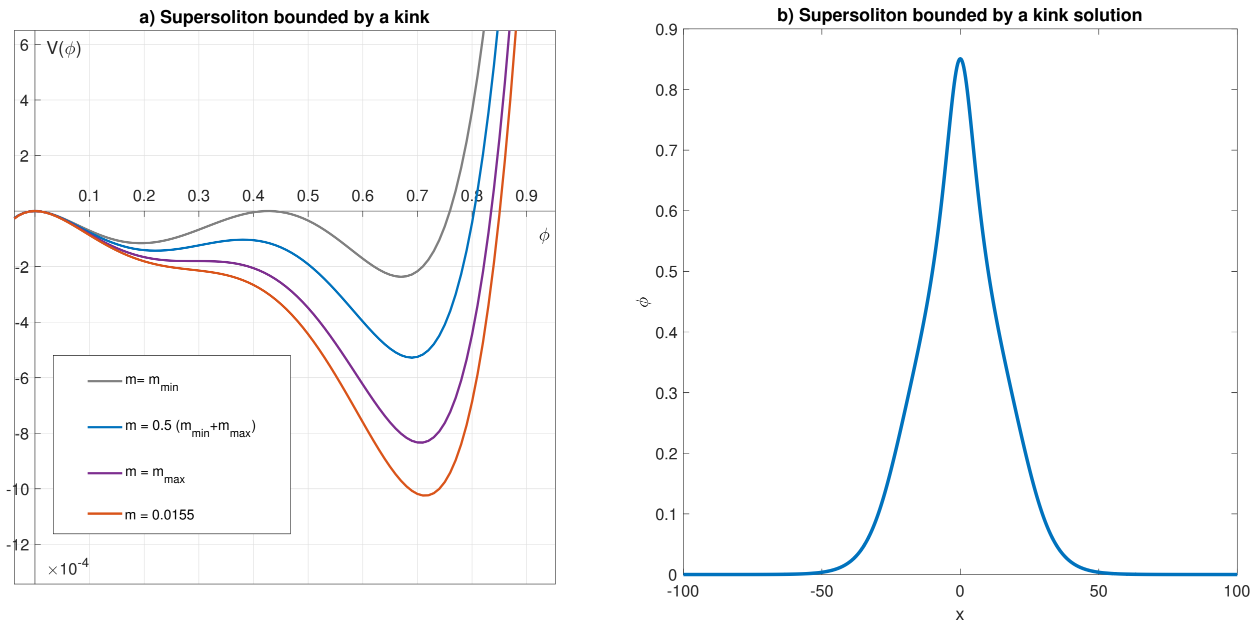

Figure 3.5: Supersoliton arise at $\theta = 2.889475$. In this figure, the supersoliton is bounded by a kink.

3.5.2 Supersoliton not bounded by a kink

In section 3.5.1, we obtained the existence of a supersoliton that formed beyond a kink solution speed and we were able to find the supersoliton speed. A kink solution does not always arise as the lower limit of supersolitons. In this case we will have to find the supersoliton directly.

To calculate the speed (m), we use the equation (3.36) to find $\Delta_3' = 0$. A cubic polynomial $P_2(\phi)$ as given in (3.62). The discriminant of a cubic polynomial P_2 is given by

$$\Delta_3' = 18ABCD - 4B^3D + B^2C^2 - 4AC^3 - 27A^2D^2 = 0. \tag{3.65}$$

Substituting A, B and C as given in (3.37) and simplifying (3.65), yields

$$\begin{aligned} m_\pm =& \frac{1}{54}\left(\left(\frac{64\cos^3\theta}{27} - 12\sin\theta\cos\theta\right)\right. \\ &\left. \pm \sqrt{\left(-\frac{64\cos^3\theta}{27} + 12\sin\theta\cos\theta\right)^2 - \left(216\sin^3\theta - 48\sin^2\theta\cos^2\theta\right)}\right). \end{aligned} \quad (3.66)$$

Therefore,

$$m_- < m < m_+. \quad (3.67)$$

The existence of a supersoliton requires the following conditions:

$$\Delta_3' = 0 \ \ and \ \ B^2 - 4AC > 0.$$

The derived Sagdeev potential is given in (3.61). The charge-neutrality at equilibrium is simply represented by the factor ϕ, while the nontrivial roots are the roots of a cubic polynomial P_2 in the bracket is given in (3.62).

For supersolitons to exist, a cubic polynomial $P_2(\phi)$ must have three distinct real roots with the same sign.
The discriminant is given by Δ_3'.

The equation of Δ_3' can be written as a quadratic equation of m as follows;

$$2700A^2m^2 + (2160ABC - 512B^3)m + 540AC^3 - 144B^2C^2 = 0. \quad (3.68)$$

We substitute A, B and C as given in (3.37) and simplify. The existence of a supersoliton depends on the existence of three non-trival roots of the potential function. Therefore, $B^2 - 4AC > 0$ that is,

$$\left(-\frac{64\cos^3\theta}{27} + 12\sin\theta\cos\theta\right)^2 - \left(216\sin^3\theta - 48\sin^2\theta\cos^2\theta\right) > 0. \quad (3.69)$$

By solving the above equation numerically, we obtain that supersolitons form without a kink whenever

$$2.863995 < \theta < \pi, \quad (3.70)$$

where $a > 0$ and $b < 0$. As an example, consider Figure 3.6 (a) where we show the behaviour of the Sagdeev potentials at $\theta = 2.873995$ for different values of the speed (m). We show the Sagdeev potential as it gives rise to a supersoliton without a kink. The blue curve shows the Sagdeev potential that arises at the minimum speed $min = 0.016973$. The red curve shows the Sagdeev potential that arises when a supersoliton occurs (intermediate) at $m = 0.5 * (min + max)$. The green curve shows the Sagdeev potential that arises below supersoliton at maximum speed $max = 0.017615$. In Figure 3.6 (b) we illustrate the solution of the modified Gardner equation. The modified Gardner equation gives rise to a supersoliton at $\theta = 2.873996$ and $m = 0.5 * (min + max)$.

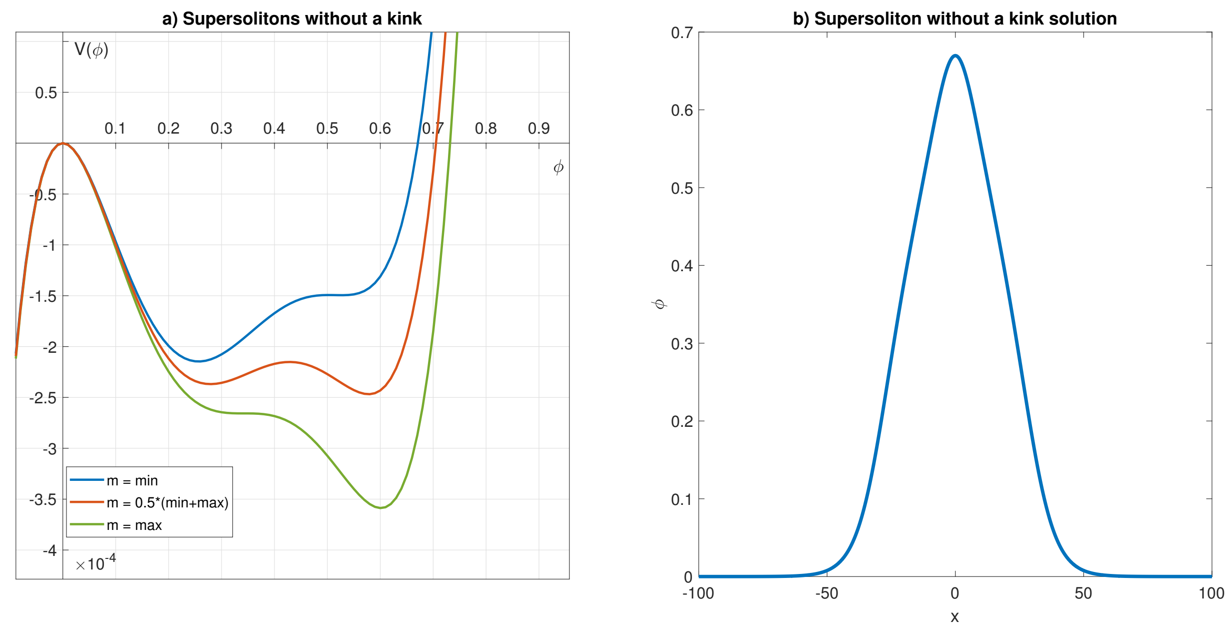

Figure 3.6: Supersoliton that arises at $\theta = 2.873996$. In this figure, the supersoliton exists without a kink.

3.6 Algebraic solution

The Sagdeev potential must have two nonzero roots, and $m = 0$ indicates that the soliton is stationary. In this case, the discriminant must be greater than zero. Algebraic solitons differ from regular solitons in two ways. Firstly, where regular solitons propagate at a fixed velocity ($m > 0$), algebraic solitons are standing waves that remain constant ($m = 0$). Secondly, the tails of regular solitons decay exponentially fast to zero when $|x| \to \infty$. In contrast, the tails of an algebraic soliton decays as a power law. This decay rate is also referred to as algebraic decay, hence the name algebraic soliton.

3.6.1 Conditions for strictly negative algebraic solution

The Sagdeev potential must have two nonzero roots. The following conditions must be met in order to obtain a negative algebraic soliton:

$m = 0$, $B^2 - 4AC > 0$, $a > 0$ and $b > 0$.

For $m = 0$, the Sagdeev potential is given in (3.39). In order to find an algebraic solution, consider

$$V(\phi) = 0. \tag{3.71}$$

This implies

$$\phi^3(C + B\phi + A\phi^2) = 0. \tag{3.72}$$

Therefore

$(\phi)^3 = 0$ (triple root) and $C + B\phi + A\phi^2 = 0$.

$$A\phi^2 + B\phi + C = 0 \tag{3.73}$$

$$\phi_\pm = \frac{-B \pm \sqrt{B^2 - 4AC}}{2A} \tag{3.74}$$

$$\phi_\pm = 5\left(-\frac{1}{6}\cos\theta \pm \sqrt{\frac{1}{36}\cos^2\theta - \frac{2}{15}\sin\theta}\right) \tag{3.75}$$

The existence of negative algebraic solutions depends on the existence of two non-trivial roots of the potential function. Therefore, $B^2 - 4AC > 0$; that is,

$$\frac{\cos^2\theta}{36} - \frac{2}{15}\sin\theta > 0. \tag{3.76}$$

The equation (3.76) can be simplified further, yielding

$$0 < \theta < \sin^{-1}\left(\frac{1}{5}\right). \tag{3.77}$$

As an example, consider Figure 3.7 where we show the Sagdeev potential that gives rise to a negative algebraic soliton at $\theta = 0.101358$ and $m = 0$. Consider Figure 3.7, where we illustrate the solution of the modified Gardner equation. The modified Gardner equation gives rise to a negative algebraic soliton at $\theta = 0.101358$ and $m = 0$.

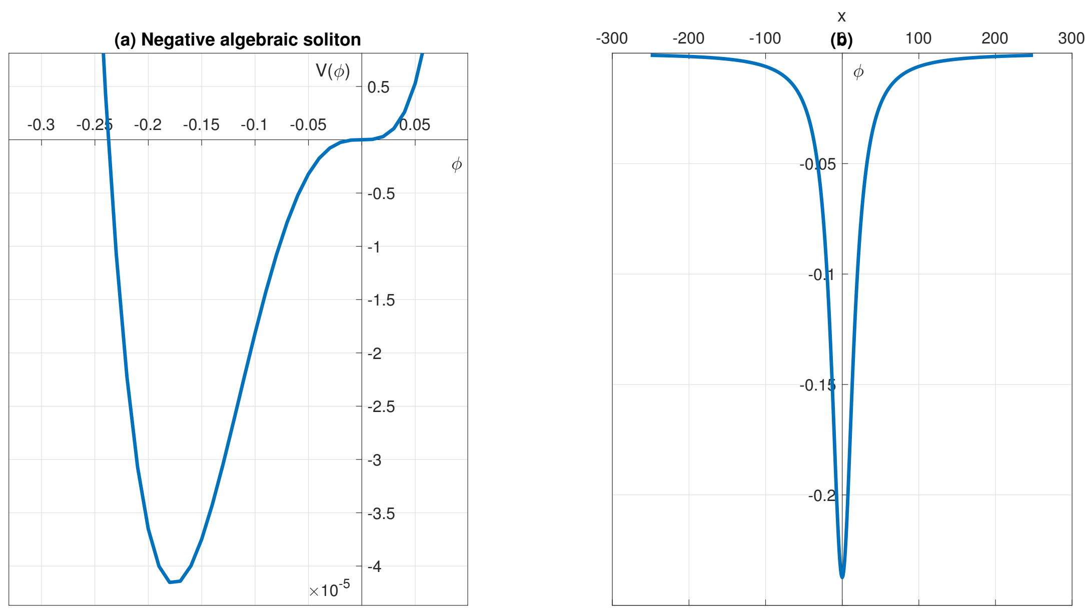

Figure 3.7: An algebraic soliton when $\theta = 0.101358$ and $m = 0$.

3.6.2 Conditions for existence of an algebraic kink

The Sagdeev potential must have a double root, and which means that the discriminant must be equal to zero. The conditions listed below must be satisfied in order to obtain an algebraic kink:

$$m = 0, \;\; b > 0, \;\; and \;\; \Delta_2 = 0,$$

with

$$\Delta_2 = B^2 = 4AC.$$

Consider the Sagdeev potential (3.39). For an algebraic kink solution to occur, $m = 0$. In order to find the roots of an algebraic kink solution, consider

$$V(\phi) = 0, \tag{3.78}$$

that is,

$$\phi^3(C + B\phi + A\phi^2) = 0. \tag{3.79}$$

Therefore

$\phi^3 = 0$ (triple root) and $C + B\phi + A\phi^2 = 0$. Solving the latter equation yields

$$\phi_{\pm} = \frac{-B \pm \sqrt{B^2 - 4AC}}{2A}, \tag{3.80}$$

that is,

$$\phi_{\pm} = 5\left(-\frac{1}{6}\cos\theta \pm \sqrt{\frac{1}{36}\cos^2\theta - \frac{2}{15}\sin\theta}\right). \tag{3.81}$$

The existence of negative algebraic kink solutions depends on the existence of two non-trival roots of the potential function. Therefore, $B^2 - 4AC = 0$; that is,

$$\frac{\cos^2\theta}{36} - \frac{2}{15}\sin\theta = 0. \tag{3.82}$$

The equation (3.82) can be simplified further yielding

$$\theta = 0.201. \tag{3.83}$$

As an example, consider Figure 3.8, where we show the Sagdeev potential at the critical speed (m) where the algebraic kink occurs at $\theta = 0.201358$ and $m = 0$. The figure shows that the double root forms at $\phi = -0.816497$.

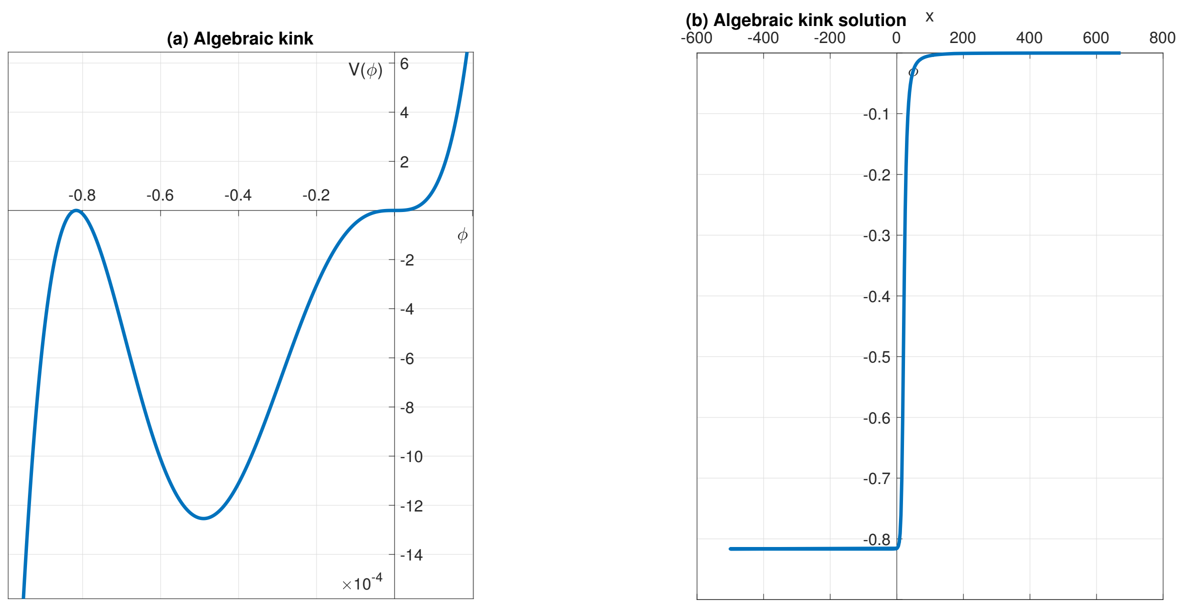

Figure 3.8: Algebraic kink when $\theta = 0.201358$ and $m = 0$.

3.6.3 Conditions for strictly positive algebraic solution

The Sagdeev potential must have two nonzero roots. The following requirements must be met in order to obtain a positive algebraic solition.

$$m = 0, \;\; B^2 - 4AC > 0 \;\; and \;\; a < 0$$

We consider the Sagdeev potential (3.39). For an algebraic solution to occur, $m = 0$. An algebraic solution is found by solving

$$V(\phi) = 0, \tag{3.84}$$

that is,

$$\phi^3(C + B\phi + A\phi^2) = 0. \tag{3.85}$$

Therefore $\phi^3 = 0$ (triple root) and $C + B\phi + A\phi^2 = 0$. Solving the latter equation leads to

$$\phi_{\pm} = \frac{-B \pm \sqrt{B^2 - 4AC}}{2A}; \tag{3.86}$$

that is,

$$\phi_{\pm} = 5\left(-\frac{1}{6}\cos\theta \pm \sqrt{\frac{1}{36}\cos^2\theta - \frac{2}{15}\sin\theta}\right) \tag{3.87}$$

The existence of positive algebraic solutions depends on the existence of two non-trivial roots of the potential function. Therefore, $B^2 - 4AC > 0$; that is,

$$\frac{\cos^2\theta}{36} - \frac{2}{15}\sin\theta > 0. \tag{3.88}$$

As mentioned earlier, $a < 0$. The equation (3.88) can be simplified further yielding

$$\pi < \theta < 2\pi. \tag{3.89}$$

For all values of satifying condition 2, condition 1 is also satisfied.

As an example, consider Figure 3.9 where we show the Sagdeev potential that gives rise to a positive algebraic soliton at $\theta = 3\pi/2$ and $m = 0$.

Consider Figure 3.9 where we show the solution of the modified Gardner equation. It gives rise to a positive algebraic soliton at $\theta = 0.101358$ and $m = 0$.

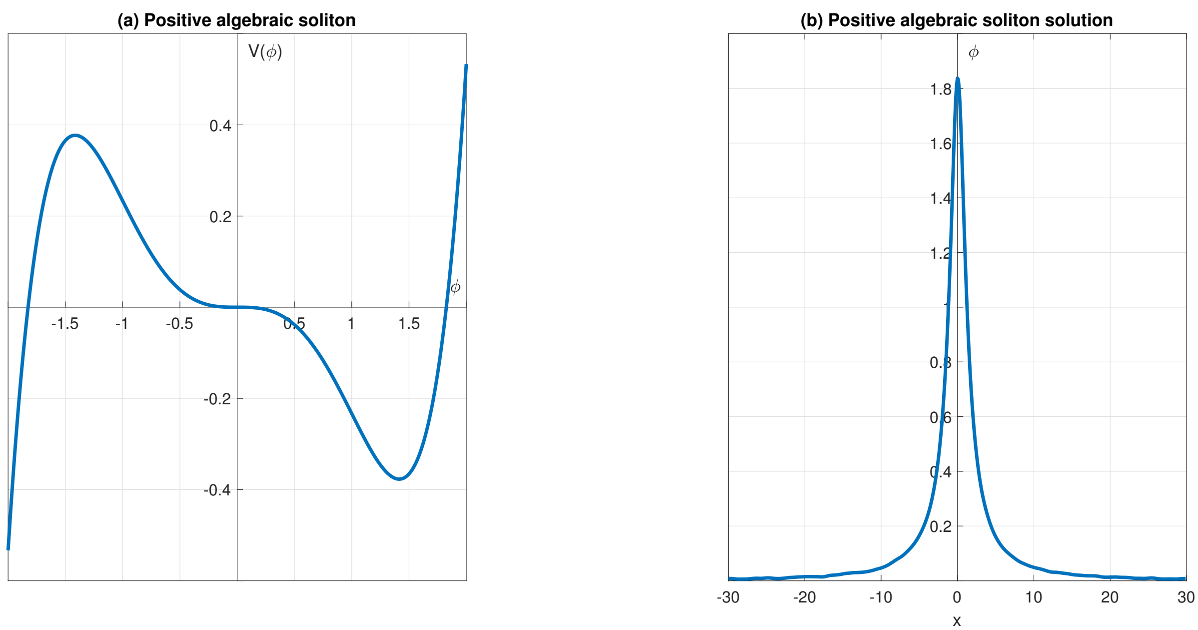

Figure 3.9: A positive algebraic soliton when $\theta = 3\pi/2$ and $m = 0$.

Chapter 4

Numerical scheme

In this chapter, we will construct the numerical methods that will be used to simulate the collision of solitons, double layers, and supersolitons for the mG equation. We begin with an examination of the periodic boundary conditions that will be used in solitons and algebraic soliton simulations. We will also go over the Neumann boundary conditions in depth because they will be used in the kink simulations. Central difference formulas will be used to approximate the $x-$derivatives.

4.1 Modified Gardner equation with periodic boundary conditions

The mG equation is given by

$$\frac{\partial \phi}{\partial t} + \frac{1}{2}\frac{\partial^3 \phi}{\partial x^3} + a\phi\frac{\partial \phi}{\partial x} + b\phi^2\frac{\partial \phi}{\partial x} + \phi^3\frac{\partial \phi}{\partial x} = 0, \tag{4.1}$$

where

$$a = \sin\theta \ \ \& \ \ b = \cos\theta.$$

In general, the spatial domain for soliton and supersoliton solutions is the entire real line. In order to simulate these solutions, we truncate the spatial domain to a large but finite interval, and apply periodic boundary conditions. Periodic boundary conditions for a function defined on the interval

$$-L/2 \leq x \leq L/2, \tag{4.2}$$

are given by $\phi(x+L,t) = \phi(x,t)$ for all x and t. The initial condition is given by $\phi(x,0) = f(x)$.

4.1.1 Semi-discretization

In order to derive a numerical scheme, we apply the so-called method of lines by initially discretizing only the spatial domain. To this end, we introduce a grid on $x \in [-L/2, L/2]$. Let $h = \frac{L}{N}$, where h is the spatial stepsize. We use $x_i = -L/2 + ih$, $i = 0, 1, \cdots, N-1$. The grid points are therefore given by $x_0 = -L/2$, $x_1 = -L/2+h$, $x_2 = -L/2 + 2h$, ...,$x_{N-1} = L/2 - h$.

We introduce the shorthand notation for function values at the grid points as follows: $\phi_i(t) = \phi(x_i, t)$.
Let's now write the boundary condition in terms of our grid. From the periodic boundary conditions, it follows that

$$\phi_i(t) = \phi_{i+N}(t). \tag{4.3}$$

The introduction of periodic conditions in a finite difference scheme then leads to

$$\begin{aligned} \phi_{-1}(t) &= \phi(-L/2 - h + L, t) && (4.4)\\ &= \phi(L/2 - h, t) && (4.5)\\ &= \phi_{N-1}(t) && (4.6) \end{aligned}$$

since $x_{N-1} = -L/2 + (N-1)L/N = L/2 - h$. Similarly,

$$\phi_N(t) = \phi(-L/2 + Nh - L, t) \tag{4.7}$$

$$= \phi(-L/2, t) \tag{4.8}$$

$$= \phi_0(t) \tag{4.9}$$

It is worth noting that $\phi_0(t) = \phi_N(t)$, so we don't need to include $\phi_N(t)$ because it is simply equal to $\phi_0(t)$. We know that $\phi_{-1}(t) = \phi_{N-1}(t)$, so we substitute $\phi_{N-1}(t)$ for $\phi_{-1}(t)$.

From central difference formulas, we approximate partial derivatives with respect to x as follows:

$$\frac{\partial \phi_i(t)}{\partial x} = \frac{\phi_{i+1}(t) - \phi_{i-1}(t)}{2h}, \tag{4.10}$$

$$\frac{\partial^3 \phi_i(t)}{\partial x^3} = \frac{\phi_{i+2}(t) - 2\phi_{i+1}(t) + 2\phi_{i-1}(t) - \phi_{i-2}(t)}{2h^3}. \tag{4.11}$$

Substituting this into the mG equation (4.1) yields the following ordinary differential equations

$$\begin{aligned}\dot{\phi_i} = \frac{\phi_{i+2} - 2\phi_{i+1+} + 2\phi_{i-1} - \phi_{i-2}}{-4h^3} - \frac{a\phi_i(\phi_{i+1} - \phi_{i-1})}{2h} - \frac{b\phi_i^2(\phi_{i+1} - \phi_{i-1})}{2h} \\ - \frac{\phi_i^3(\phi_{i+1} - \phi_{i-1})}{2h},\end{aligned} \tag{4.12}$$

for $i = 0, 1, 2, ..., N-1$. For $i = 0$, we know that

$$\phi_0(t) = \phi_{0+N}(t) = \phi_N(t). \tag{4.13}$$

Similarily,

$$\phi_{-1}(t) = \phi_{N-1}(t), \tag{4.14}$$

for $i = N-1$. Therefore

$$\frac{\partial \phi_{N-1}(t)}{\partial x} = \frac{\phi_0(t) - \phi_{N-2}(t)}{2h}, \tag{4.15}$$

since

$$\phi_0(t) = \phi_N(t). \tag{4.16}$$

Similarly at $i = 0$, one gets that

$$\begin{aligned}\dot{\phi}_0 = &-\frac{\phi_2 - 2\phi_1 + 2\phi_{N-1} - \phi_{N-2}}{4h^3} - a\frac{\phi_0(\phi_1 - \phi_{N-1})}{2h} \\ &- b\frac{\phi_0^2(\phi_1 - \phi_{N-1})}{2h} - \frac{\phi_0^3(\phi_1 - \phi_{N-1})}{2h}.\end{aligned} \tag{4.17}$$

For the boundary point at $i = 1$, we obtain

$$\begin{aligned}\dot{\phi}_1 = &-\frac{\phi_3 - 2\phi_2 + 2\phi_0 - \phi_{N-1}}{4h^3} - a\frac{\phi_1(\phi_2 - \phi_0)}{2h} - b\frac{\phi_1^2(\phi_2 - \phi_0)}{2h} \\ &- \frac{\phi_1^3(\phi_2 - \phi_0)}{2h},\end{aligned} \tag{4.18}$$

the equation at $i = N - 2$ yields

$$\begin{aligned}\dot{\phi}_{N-2} = &\frac{\phi_0 - 2\phi_{N-1} + 2\phi_{N-3} - \phi_{N-4}}{4h^3} - a\frac{\phi_{N-2}(\phi_{N-1} - \phi_{N-3})}{2h} \\ &- b\frac{\phi_{N-2}^2(\phi_{N-1} - \phi_{N-3})}{2h} - \frac{\phi_{N-2}^3(\phi_{N-1} - \phi_{N-3})}{2h}.\end{aligned} \tag{4.19}$$

Finally, for the boundary point at $i = N - 1$, gives

$$\begin{aligned}\dot{\phi}_{N-1} = &-\frac{\phi_1 - 2\phi_0 + 2\phi_{N-2} - \phi_{N-3}}{4h^3} - a\frac{\phi_{N-1}(\phi_0 - \phi_{N-2})}{2h} - b\frac{\phi_{N-1}^2(\phi_0 - \phi_{N-2})}{2h} \\ &- \frac{\phi_{N-1}^3(\phi_0 - \phi_{N-2})}{2h}.\end{aligned} \tag{4.20}$$

The semi-discretization of the mG equation then yields a system of first-order ordinary differential equations of the form

$$\dot{\Theta} = F(\Theta), \tag{4.21}$$

where Θ can be expressed in the form

$$\Theta(t) = \begin{bmatrix} \phi_0(t) \\ \phi_1(t) \\ \vdots \\ \phi_{N-2}(t) \\ \phi_{N-1}(t) \end{bmatrix},$$

$$F(\Theta) = \begin{bmatrix} (-\phi_2 - 2\phi_1 + 2\phi_{N-1} - \phi_{N-2})/4h^3 - (a\phi_0 + b\phi_0^2 + \phi_0^3)(\phi_1 - \phi_{N-1})/(2h) \\ (-\phi_3 - 2\phi_2 + 2\phi_0 - \phi_{N-1})/4h^3 - (a\phi_1 + b\phi_1^2 + \phi_1^3)(\phi_2 - \phi_0)/(2h) \\ \vdots \\ (\phi_0 - 2\phi_{N-1} + 2\phi_{N-3} - \phi_{N-4})/4h^3 - (a\phi_{N-2} + b\phi_{N-2}^2 + \phi_{N-2}^3)(\phi_{N-1} - \phi_{N-3})/(2h) \\ (-\phi_1 - 2\phi_0 + 2\phi_{N-2} - \phi_{N-3})/4h^3 - (a\phi_{N-1} + b\phi_{N-1}^2 + \phi_{N-1}^3)(\phi_0 - \phi_{N-2})/(2h) \end{bmatrix}.$$

$\phi_i(0) = f(x_i)$, obtained in the initial condition for $i = 0, 1, ..., N-1$. Since the semi-discretized equations yield a system of ODEs, we now proceed with the last step of the method, namely the discretization of the time variable. To this end, let $t_j = jq$ where q is the time step. Let

$$\Theta^{(j)} = \Theta(t_j) = \begin{bmatrix} \phi_{0,j} \\ \phi_{1,j} \\ \vdots \\ \phi_{N-1,j} \end{bmatrix}$$

where $\phi_{ij} = \phi(x_i, t_j)$.

The resulting initial value problem can be resolved using the fourth order Runge-kutta method. The fourth-order Runge-Kutta method is given by

$$\Theta^{(j+1)} = \Theta^{(j)} + \frac{1}{6}(k_1 + 2k_2 + 2k_3 + k_4) \tag{4.22}$$

where

$$k_1 = qF(\Theta^{(j)}),$$

$$k_2 = qF(\Theta^{(j)} + \frac{1}{2}k_1),$$
$$k_3 = qF(\Theta^{(j)} + \frac{1}{2}k_2),$$
$$k_4 = qF(\Theta^{(j)} + k_3).$$

4.2 Modified Gardner equation with Neumann boundary conditions

We consider the mG equation given in (4.1). In general, the spatial domain for kink solutions is the entire real line. In order to simulate the solution, we truncate the spatial domain to a large but finite interval and apply Neumann boundary conditions. Neumann boundary conditions for a function defined on the interval given in (4.2), with boundary conditions are given as follows:

At $x = -L/2$, we have

$$\frac{\partial \phi}{\partial x}(-L/2, t) = \frac{\partial^2 \phi}{\partial x^2}(-L/2, t) = 0. \tag{4.23}$$

At $x = L/2$

$$\frac{\partial \phi}{\partial x}(L/2, t) = \frac{\partial^2 \phi}{\partial x^2}(L/2, t) = 0. \tag{4.24}$$

The initial condition is given by
$\phi(x, 0) = f(x)$.

4.2.1 Semi-discretization

We use the same method used in periodic boundary conditions to derive a numerical scheme. We also introduce same grid as a periodic boundary conditions. In this case $x_i = -L/2 + ih$, for $i = 1, 2, ..., N-1$ where is the interval length given by $h = \frac{L}{N}$.

From the boundary conditions, we know that at boundary point $i = 0$

$$\frac{\partial \phi}{\partial x}(-L/2, t) = \frac{\partial \phi_0(t)}{\partial x} = 0. \tag{4.25}$$

From the central difference method, we approximate this derivative, to obtain

$$\frac{\phi_1(t) - \phi_{-1}(t)}{2h} = 0. \tag{4.26}$$

Solving $\phi_{-1,t}$, one obtains the approximation

$$\phi_{-1}(t) = \phi_1(t), \tag{4.27}$$

One can apply a similar procedure to the boundary condition on the right-hand side for we know that $x_N = L/2$. At the boundary $i = N$,

$$\frac{\partial \phi}{\partial x}(L/2, t) = \frac{\phi_{N+1}(t) - \phi_{N-1}(t)}{2h} = 0. \tag{4.28}$$

Solving $\phi_{N+1}(t)$, one obtains the approximation

$$\phi_{N+1}(t) = \phi_{N-1}(t). \tag{4.29}$$

Since

$$\frac{\partial \phi_0(t)}{\partial x} = 0, \tag{4.30}$$

we know that

$$\frac{\partial^2 \phi_0(t)}{\partial x^2} = \frac{\phi_{0+1}(t) - 2\phi_0(t) + \phi_{0-1}(t)}{h^2} = 0 \tag{4.31}$$

one obtains the approximation

$$\phi_1(t) = \phi_0(t). \tag{4.32}$$

Applying a similar procedure

$$\frac{\partial^2 \phi_N(t)}{\partial x^2} = 0, \tag{4.33}$$

one obtains the approximation,

$$\phi_{N-1}(t) = \phi_N(t). \tag{4.34}$$

A similar approach as periodic boundary conditions is now applied. We approximate partial derivatives with respect to x using central difference formulas, which are

(4.10) and (4.11). Substituting (4.10) and (4.11) into the mG equation (4.1) yields the system of ODEs given by (4.12).

For Neumann boundary conditions, the first boundary point occurs at $i = 1$, as compared with the periodic, which began at $i = 0$. We now have

$$\begin{aligned}\dot{\phi}_1 = &-\frac{\phi_3 - 2\phi_2 + 2\phi_1 - \phi_1}{4h^3} - \frac{a\phi_1(\phi_2 - \phi_1)}{2h} \\ &- b\frac{\phi_1^2(\phi_2 - \phi_1)}{2h} - \frac{\phi_1^3(\phi_2 - \phi_1)}{2h},\end{aligned} \tag{4.35}$$

since $\phi_0(t) = \phi_1(t)$.

The boundary at $i = 2$ gives

$$\begin{aligned}\dot{\phi}_2 = &-\frac{\phi_4 - 2\phi_3 + 2\phi_1 - \phi_1}{4h^3} - \frac{a\phi_2(\phi_3 - \phi_1)}{2h} - \frac{b\phi_2^2(\phi_3 - \phi_1)}{2h} \\ &- \frac{\phi_2^3(\phi_3 - \phi_1)}{2h},\end{aligned} \tag{4.36}$$

while the equation at $i = N - 2$ yields

$$\begin{aligned}\dot{\phi}_{N-2} = &-\frac{\phi_{N-1} - 2\phi_{N-1} + 2\phi_{N-3} - \phi_{N-4}}{4h^3} - \frac{a\phi_{N-2}(\phi_{N-1} - \phi_{N-3})}{2h} \\ &- \frac{b\phi_{N-2}^2(\phi_{N-1} - \phi_{N-3})}{2h} - \frac{\phi_{N-2}^3(\phi_{N-1} - \phi_{N-3})}{2h}.\end{aligned} \tag{4.37}$$

Finally, for $i = N - 1$, one gets

$$\begin{aligned}\dot{\phi}_{N-1} = &-\frac{\phi_{N-1} - 2\phi_{N-1} + 2\phi_{N-2} - \phi_{N-3}}{4h^3} - \frac{a\phi_{N-1}(\phi_{N-1} - \phi_{N-2})}{2h} - \frac{b\phi_{N-1}^2(\phi_{N-1} - \phi_{N-2})}{2h} \\ &- \frac{\phi_{N-1}^3(\phi_{N-1} - \phi_{N-2})}{2h}.\end{aligned} \tag{4.38}$$

The semi-discretization of the mG equation results in a system of first-order ordinary differential equations (4.21) in which Θ can be expressed similarly to the periodic boundary conditions. The difference is that first boundary point at periodic occurs at $i = 0$ whereas at Neumann initial boundary point occurs at $i = 1$. We have that

$$\Theta(t) = \begin{bmatrix} \phi_1(t) \\ \phi_2(t) \\ \vdots \\ \phi_{N-2}(t) \\ \phi_{N-1}(t) \end{bmatrix},$$

$$F(\Theta) = \begin{bmatrix} (-\phi_3 - 2\phi_2 + 2\phi_1 - \phi_1)/4h^3 - (a\phi_1 + b\phi_1^2 + \phi_1^3)(\phi_2 - \phi_1)/(2h) \\ (-\phi_4 - 2\phi_3 + 2\phi_1 - \phi_1)/4h^3 - (a\phi_2 + b\phi_2^2 + \phi_2^3)(\phi_3 - \phi_1)/(2h) \\ \vdots \\ (-\phi_{N-1} - 2\phi_{N-1} + 2\phi_{N-3} - \phi_{N-4})/4h^3 - (a\phi_{N-2} + b\phi_{N-2}^2 + \phi_{N-2}^3)(\phi_{N-1} - \phi_{N-3})/(2h) \\ (-\phi_{N-1} - 2\phi_{N-1} + 2\phi_{N-2} - \phi_{N-3})/4h^3 - (a\phi_{N-1} + b\phi_{N-1}^2 + \phi_{N-1}^3)(\phi_{N-1} - \phi_{N-2})/(2h) \end{bmatrix}.$$

Note that $\phi_i(0) = f(x_i)$, obtained in the initial condition for $i = 1, 2......, N-1$. The discretization of the time variable is similar to that given in periodic boundary conditions. The key difference is the starting point. As stated in the periodic boundary conditions, $t_j = jq$. In this particular case, we have

$$\Theta^{(j)} = \Theta(t_j) = \begin{bmatrix} \phi_{1,j} \\ \phi_{2,j} \\ \vdots \\ \phi_{N-1,j} \end{bmatrix}$$

where $\phi_{ij} = \phi(x_i, t_j)$.

The resulting initial value problem can be solved using the fourth order Runge-Kutta method. We consider the Runge-Kutta method as given in the periodic boundary conditions by (4.22).

4.3 Constructing the initial condition

To simulate collisions between solitons and supersolitons, solutions must be constructed on a suitably large interval. The numerical integration is not accurate enough to provide such solutions due to the instability of the energy like integral (3.34). We focus on only the tail of the soliton/supersoliton, so that we are restricted to small disturbances in the electrostatic potential. Our strategy is to apply a Taylor series expansion to obtain a straightforward formula for the Sagdeev potential close to equilibrium. By substituting this expression into the energy integral and integrating, we can derive an analytical expression for the soliton/supersolitons' tails. The energy like integral defined in (3.34), is as follows

$$\frac{1}{2}(\frac{d\phi}{d\xi})^2 + V(\phi, m) = 0. \tag{4.39}$$

As a result, we construct sufficiently long tails for the solutions. We employ the ideas of Olivier et al. [43] where the asymptotic behaviour of solitons and double layers was analyzed. A Taylor series expansion is used to derive the asymptotic behaviour using the Sagdeev pseudopotential approach. We only need to consider the shape of the Sagdeev potential $V(\phi, m)$ near the equilibrium electrostatic potential $\phi = 0$. Our method relies on a Taylor series expansion to the so$-$called Sagdeev potential to obtain a simple expression for the Sagdeev potential near the equilibrium.

A Taylor series expansion is used to derive the asymptotic behaviour. The first step is to apply a Taylor series expansion of the function $V(\phi, m)$ about the equilibrium density $\phi = 0$. The Sagdeev potential satisfies $V(0, M) = 0$ and $\partial V/\partial\phi(0, m) = 0$ due to boundary conditions. This implies that a Taylor series' lowest-order terms expanded about the equilibrium potential $\phi = 0$

$$V(\phi, m) = X(m)\phi^2 + Y(m)\phi^3 + \mathcal{O}(\phi^4). \tag{4.40}$$

The values of the constants are as follows

$$X(m) = \frac{1}{2}\frac{\partial^2 V}{\partial\phi^2}(0, m), \;\; Y(m) = \frac{1}{6}\frac{\partial^3 V}{\partial\phi^3}(0, m). \tag{4.41}$$

4.3.1 Constructing the initial conditions for a regular soliton and supersoliton

For a regular soliton $m \neq 0$. ϕ must be sufficiently small for the approximations to be accurate. In this case, we take the lowest-order approximation ϕ^2 into account. Contributions of the order ϕ^3 and higher are sufficiently small to be treated as negligible. To investigate the tail of a regular soliton governed by the properties of the Sagdeev potential at the root ϕ_r, we can expand the Sagdeev potential about the root $\phi_r = 0$

$$V(\phi) = V(0) + (\phi)V'(\phi_r) + \frac{(\phi)^2}{2}V''(0) + ... \tag{4.42}$$

$\phi_r = 0$, as we only need to analyze the shape of the Sagdeev potential near the equilibrium electrostatic potential. We use primes to denote partial derivatives with respect to ϕ. It should be noted that the Sagdeev potential satisfies

$$V(0, m) = \frac{\partial V}{\partial \phi}(0, m) = 0. \tag{4.43}$$

As a result, the first two terms in the series disappear. The resulting Taylor series expansion can be approximated as

$$V(\phi) \approx \frac{(\phi)^2}{2}V''(0), \tag{4.44}$$

where

$$V''(0) = -2m. \tag{4.45}$$

Let $U = -2m$. As shown below, we have the energy as an integral.

$$\frac{1}{2}(\frac{d\phi}{d\xi})^2 + V(\phi) = 0. \tag{4.46}$$

After substitution, we get

$$\frac{1}{2}(\frac{d\phi}{d\xi})^2 + \frac{\phi^2}{2}U = 0. \tag{4.47}$$

This can be reduced to the differential equation

$$\frac{d\phi}{d\xi} = \pm\sqrt{-(\phi)^2 U}. \tag{4.48}$$

Equation (4.48) can be written as a separable equation, then integrated and simplified to produce

$$\phi = C \exp^{\pm\sqrt{2m}\xi}. \tag{4.49}$$

Due to the symmetry of the solutions, we only consider the tail on the interval $\xi > 0$. To this end, we use the upper positive sign for negative solitons and the lower negative sign for positive solitons. When we solve for C, we get the following result:

$$C = \phi \exp^{\pm\sqrt{2m}\xi}. \tag{4.50}$$

We conduct a similar analysis for a supersoliton because $m \neq 0$.

4.3.2 Constructing the initial conditions for a positive and negative kink

For the approximations to be accurate, ϕ must be sufficiently small. In this case, we consider the lowest-order approximation ϕ^2. The contributions of the order ϕ^3 and higher are negligible. To investigate a kink solution's tail governed by the properties of the Sagdeev potential at the root ϕ_r, we can expand the Sagdeev potential about the kink root $\phi = \phi_r$ to obtain

$$V(\phi) = V(\phi_r) + (\phi - \phi_r)V'(\phi_r) + \frac{(\phi - \phi_r)^2}{2}V''(\phi_r) + ... \tag{4.51}$$

Note that the Sagdeev potential satisfies $V(0, m) = \partial V/\partial\phi(0, m) = 0$. Therefore, the first two terms in the series vanish. As a result, we can simplify the Taylor series expansion to the form

$$V(\phi) \approx \frac{(\phi - \phi_r)^2}{2}V''(\phi_r), \tag{4.52}$$

where

$$V''(\phi_r) = 2\phi_r^3 + 2b\phi_r^2 + 2a\phi_r - 2m. \tag{4.53}$$

Let $U = 2\phi_r^3 + 2b\phi_r^2 + 2a\phi_r - 2m$. A kink is usually associated with a double root at ϕ_r. We have the energy like integral as follows

$$\frac{1}{2}(\frac{d\phi}{d\xi})^2 + V(\phi) = 0. \tag{4.54}$$

This can be simplified to yield the differential equation shown below

$$\frac{d\phi}{d\xi} = \pm\sqrt{-(\phi - \phi_r)^2 U}. \tag{4.55}$$

Equation (4.55) can be written as a separable equation, and then the equation can be integrated and simplified to yield the following results

$$\phi = C \exp^{\pm\sqrt{-U}\xi} + \phi_r. \tag{4.56}$$

The kink solution exists under two conditions, $\phi \to \phi_r$ when $\xi \to -\infty$ and $\phi \to 0$ when $\xi \to +\infty$. We set $\phi(0) = \phi_r \pm 10^{-4}$, so that

$$\phi_r \pm 10^{-4} = Ce^0 + \phi_r, \tag{4.57}$$

where the upper positive sign is used for negative kinks with $\phi_r < 0$, and the lower negative sign is used for positive kinks with $\phi_r > 0$. When we simplify expression (4.57), we get

$$C = \pm 10^{-4}, \tag{4.58}$$

where the upper positive sign is used for negative kinks and the lower negative sign is used for positive kinks. Second condition, ϕ' at $\xi = 0$

$$\phi'(0) = C \pm \sqrt{(-U)}. \tag{4.59}$$

For a kink solution's tail governed by the properties of the Sagdeev potential at the origin $\phi = 0$, we perform the same analysis as in subsection (4.3.1) and obtain the solution.

$$\phi = C \exp^{\pm\sqrt{2m}\xi}. \tag{4.60}$$

The only difference between a regular soliton and kinks is that the signs are reversed, as the limit of ξ in kinks goes to $-\infty$.

After constructing the appropriate initial condition, the fourth-order Runge-Kutta method is used to solve the energy integral equation numerically. In summary, a double layer solution's two tails are determined by the properties of the Sagdeev potentials at the double root $\phi = \phi_r$ and at the origin $\phi = 0$.

4.3.3 Constructing the initial conditions for algebraic soliton

For an algebraic soliton $m = 0$. Consider ϕ to be sufficiently small. In this case, we consider the lowest order term of the Sagdeev potential of the order ϕ^3. To investigate the tail's asymptotic behavior, we can expand the Sagdeev potential about the root $\phi = 0$ to obtain

$$V(\phi) = V(0) + (\phi - 0)V'(0) + \frac{(\phi - 0)^2}{2}V''(0) + \frac{(\phi - 0)^3}{6}V'''.... \tag{4.61}$$

Note that the Sagdeev potential satisfies, $m = 0$ and $V(0) = \partial V/\partial\phi(0) = \partial^2 V/\partial\phi^2(0) = 0$. Therefore, the first three terms in the series vanish. As a result, we can simplify the Taylor series expansion to the form

$$V(\phi) \approx \frac{\phi^3}{6}V'''(0), \tag{4.62}$$

where

$$V'''(0) = 2a. \tag{4.63}$$

We have the energy integral

$$\frac{1}{2}(\frac{d\phi}{d\xi})^2 + \frac{a}{3}\phi^3 = 0. \tag{4.64}$$

We follow a similar treatment performed in the regular solitons' tails, obtaining a negative algebraic soliton as follows

$$\phi = \frac{-4}{\left(\pm\sqrt{\frac{2a}{3}}\xi + C\right)^2}. \tag{4.65}$$

Tails for the negative algebraic soliton are constructed under condition, $\phi(0) = -10^{-4}$. When we solve for C, we get the following result:

$$C = \pm\sqrt{\frac{4}{10^{-4}}}, \tag{4.66}$$

where the lower negative sign denotes negative algebraic soliton.

For a positive algebraic soliton,

$$\phi = \frac{4}{\left(\pm\sqrt{\frac{-2a}{3}}\xi + C\right)^2}. \tag{4.67}$$

Tails for the positive algebraic soliton are constructed under condition, $\phi(0) = 10^{-4}$. When we solve for C, we get the following result:

$$C = \pm\sqrt{\frac{4}{10^{-4}}}, \tag{4.68}$$

where the upper positive sign denotes the positive algebraic soliton.

4.3.4 Constructing the initial conditions for an algebraic kink

To investigate an algebraic kink's tail governed by the properties of the Sagdeev potential at the root ϕ_r, we can expand the Sagdeev potential about the root $\phi = \phi_r$ to obtain

$$V(\phi) = V(\phi_r) + (\phi - \phi_r)V'(\phi_r) + \frac{(\phi - \phi_r)^2}{2}V''(\phi_r) + ... \tag{4.69}$$

Note that the Sagdeev potential satisfies $V(0, m) = \partial V/\partial\phi(0, m) = 0$. Therefore, the first two terms in the series vanish. As a result, we can simplify the Taylor series expansion to the form

$$V(\phi) \approx \frac{(\phi - \phi_r)^2}{2}V''(\phi_r), \tag{4.70}$$

where

$$V''(\phi_r) = 2\phi_r^2 + 2b\phi_r^2 + 2a\phi_r - 2m. \tag{4.71}$$

Let $U = 2\phi_r^2 + 2b\phi_r^2 + 2a\phi_r - 2m$. We have the energy like integral as follows

$$\frac{1}{2}(\frac{d\phi}{d\xi})^2 + V(\phi) = 0. \tag{4.72}$$

This can be simplified to yield the differential equation

$$\frac{d\phi}{d\xi} = \pm\sqrt{-\frac{2(\phi - \phi_r)^2}{2}U}. \tag{4.73}$$

Equation (4.73) can be written as a separable equation, and then the equation can be integrated and simplified to yield

$$\phi = C \exp^{\pm\sqrt{-U}\xi} + \phi_r. \tag{4.74}$$

The tail of the algebraic kink solution is constructed subject to the following condition at $\xi = 0$

$$\phi - 10^{-4} = Ce^0 + \phi_r. \tag{4.75}$$

When we simplify expression (4.75), we get

$$C = 10^{-4}. \tag{4.76}$$

A second condition, at $\xi = 0$ is then given by

$$\phi'(0) = C \pm \sqrt{(-U)}. \tag{4.77}$$

For an algebraic kink's tail governed by the properties of the Sagdeev potential at the origin $\phi = 0$, we can expand the Sagdeev potential about the origin. To investigate the tail's asymptotic behavior, we can expand the Sagdeev potential about the root $\phi = 0$ to obtain

$$V(\phi) = V(0) + (\phi - 0)V'(0) + \frac{(\phi - 0)^2}{2}V''(0) + \frac{(\phi - 0)^3}{6}V'''(0).... \tag{4.78}$$

Note that the Sagdeev potential satisfies, $m = 0$ and $V'(0) = 0$. Therefore, the first three terms in the series vanish. As a result, we can simplify the Taylor series expansion to the form

$$V(\phi) \approx \frac{(\phi)^3}{6}V'''(0), \tag{4.79}$$

where

$$V'''(0) = 2a. \tag{4.80}$$

We have the energy integral as follows

$$\frac{1}{2}(\frac{d\phi}{d\xi})^2 + \frac{a}{3}\phi^3 = 0. \tag{4.81}$$

Following a similar treatment performed in the kink's tails, one obtains a negative algebraic solution as follows

$$\phi = \frac{-4}{\left(\pm\sqrt{\frac{2a}{3}}\xi + C\right)^2}. \tag{4.82}$$

Then

$$C = \sqrt{\frac{-4}{\phi_0}} \pm \sqrt{\frac{2a}{3}}\xi. \tag{4.83}$$

Chapter 5

Results

After constructing the numerical methods that will be used to simulate the collision of solitons, double layers, and supersolitons for the mG equation in the previous chapter, we now simulate collision properties of solitons overtaking nonlinear waves in the modified Gardner equation, such as algebraic solitons and kink solutions. We start by numerically integrating the energy equation. The findings are represented graphically.

5.1 Collision of two positive solitons

For the mG equation, we can simulate collision between two solitons. To achieve this, we numerically integrate the energy equation defined in (3.34) and create a faster positive soliton and a slower positive soliton. We start off by combining these two initial conditions by shifting the faster soliton 50 to the left far enough from the slower soliton. We will compare the solutions as we increase in time T for $0 \leq T \leq 3000$. We make h and k sufficiently small, where $h = 0.1$, $k = 0.0001$, $N = 3000$, $L = 300$, $\theta = 1.047198$. The speed of the faster soliton is $m = 1$ and the speed of the slower soliton is $m = 0.5$. The collision of the resulting two solitons is shown in Figure 5.1 below. The figure shows the magnitude of the solution ϕ is plotted as a function of T and ξ. The faster soliton is initially on the left, while the slower soliton is initially on the right. We can see that after collision, solitons maintain their shapes but it is clearer in Figure 5.2 as we show different solutions as T increases.

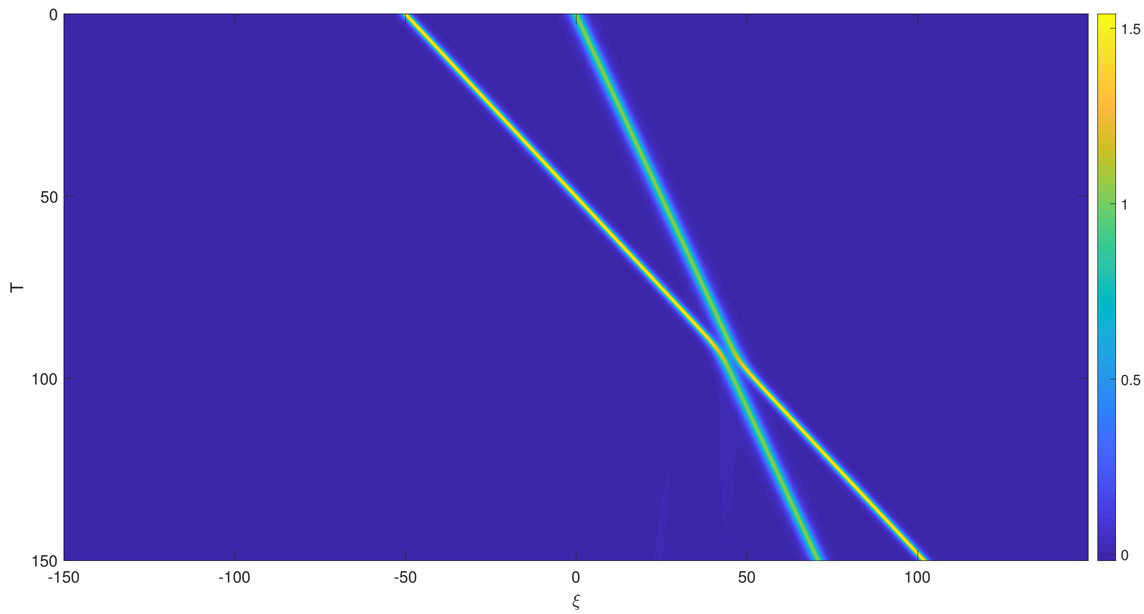

Figure 5.1: A faster soliton overtakes a slower soliton in this simulation. The electrostatic potential ϕ is plotted as a function of T and ξ.

Consider Figure 5.2, where we show the solution for six different values of T. We plotted electrostatic potential ϕ versus variable x, where the faster soliton overtakes a slower soliton. The collision of the resulting two solitons is shown in Figure 5.2. Initially, at $T = 0$ the faster soliton is shifted 50 units to the left and then added to a slower soliton solution that begins at the origin. As shown at $T = 80$ and $T = 100$, the faster soliton overtakes the slower soliton. The two solitons maintain their shapes after collision. As T increases, the faster soliton moves further ahead and the slower soliton moves further behind. In conclusion to this case, collision is inelastic.

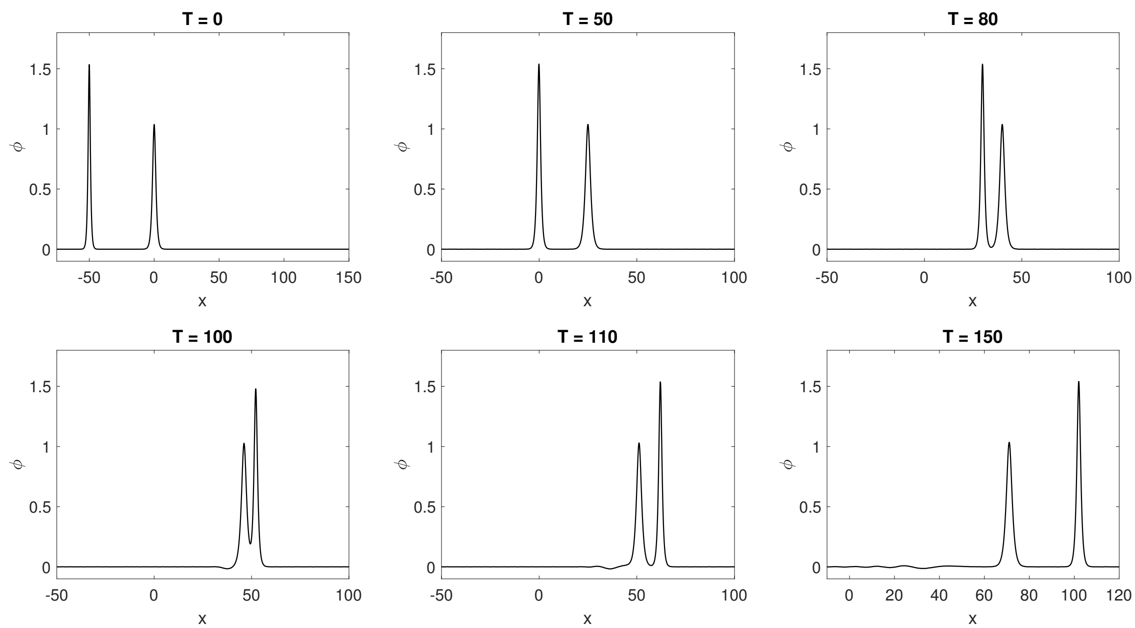

Figure 5.2: A faster soliton overtaking a slower soliton.

Based on the findings of Zabusky and Kruskal [1], they conducted a simulation study of overtaking collisions between between faster and slower solitons of KdV. According to the findings, except for a phase shift, slower and faster solitons collide and then emerge from the collision unchanged. Our simulation results does not agree with Zabusky and Kruskal's observations from 1965.

5.2 Collision between positive and negative solitons

Second, we simulate collision between a negative and a positive soliton. The speed of the negative soliton is $m = 0.1$ and the speed of postive soliton is $m = 0.4$, with $N = 2000$, $L = 100$, $k = 0.00001$ and $\theta = -1.370796$. The collision of the resulting two solitons is shown in Figure 5.3 and Figure 5.4.

Consider Figure 5.3, which depicts the values of the solution ϕ as a function of T and ξ. The faster soliton starts on the left, while the slower soliton starts on the right. We can see that solitons retain their shapes after collision, but it is clearer in figure 5.4 where we show various solutions as T increases.

Consider Figure 5.4, which shows the solution for six different values of T. Initially, at $T = 0$ the positive soliton is shifted 25 units to the left and then added to a negative soliton solution that begins at the origin. As shown at $T = 50$, $T = 60$ and $T = 80$, the positive soliton overtakes the negative soliton. The two solitons maintain their shapes after collision. As T increases, the positive soliton moves further ahead and the negative soliton moves further behind.

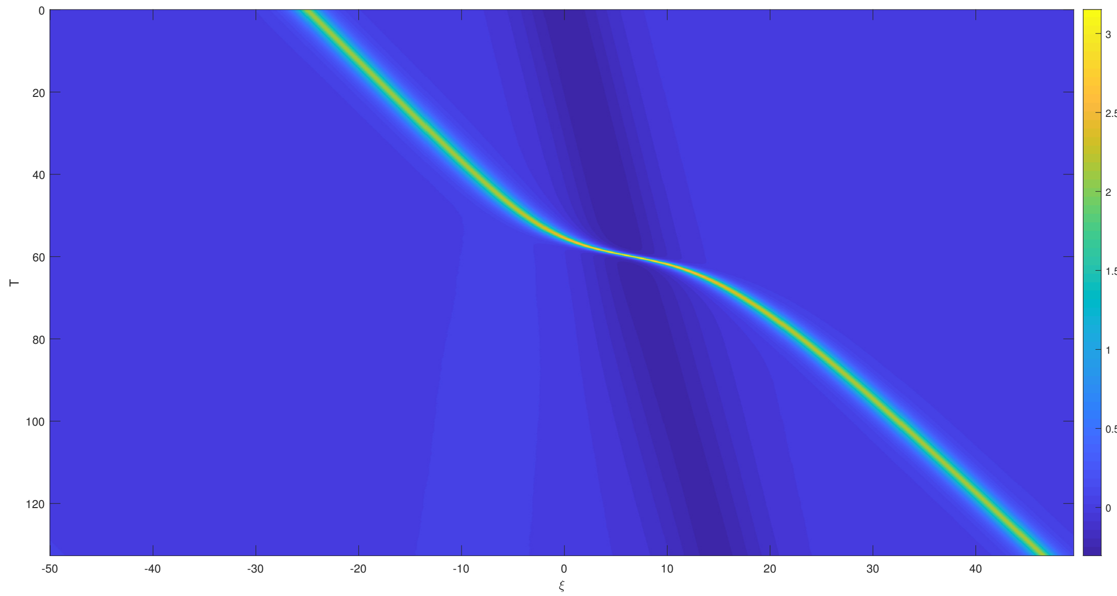

Figure 5.3: A positive soliton (yellow) is simulated overtaking a negative soliton (dark blue). The electrostatic potential ϕ as a function of T and ξ is plotted.

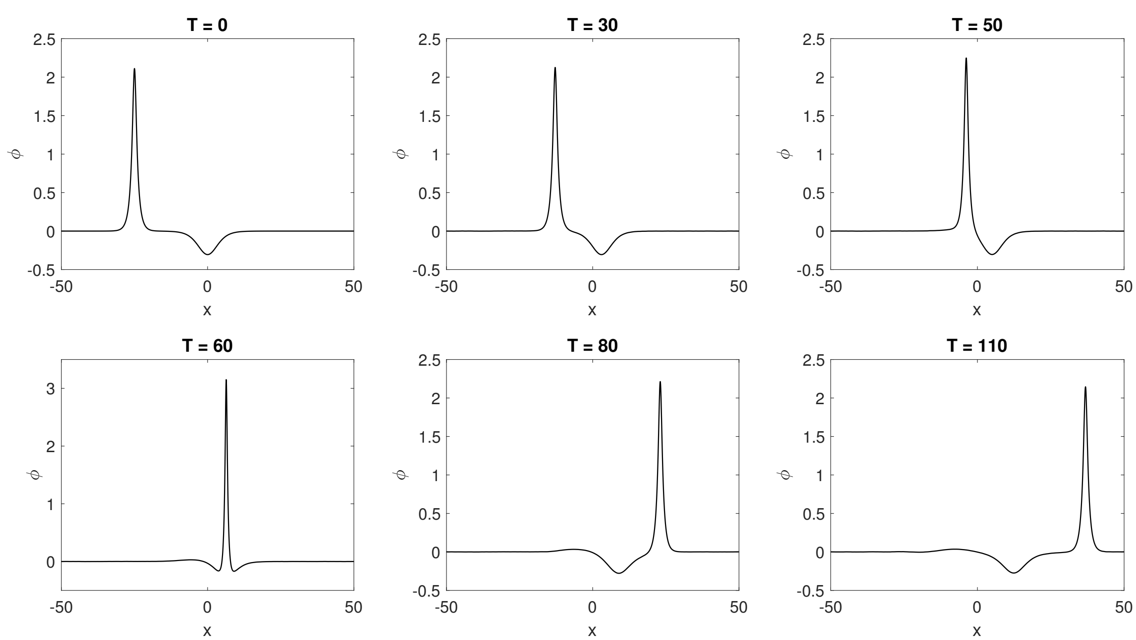

Figure 5.4: Snapshots of a positive soliton overtaking a negative soliton. We plotted electrostatic potential ϕ at various T values.

The collision is inelastic, which is the same results we received when a positive soliton overtakes another positive soliton.

5.3 Collision between negative kink and negative soliton

Third, we simulate collision between a negative soliton and a negative kink solution. To simulate a collision, we combine these two initial conditions by shifting the soliton initial condition far away from the kink's center. The speed of the kink is $m = 0.267$ and the speed of the negative soliton is $m = 0.1$, with $N = 6000$, $L = 600$, $h = 0.1$, $k = 0.0001$ and $\theta = -1.370796$. The collision of the resulting solutions is shown in Figure 5.5 and Figure 5.6. The solution for different values of T is shown in the Figure 5.6.

Consider figure 5.5, where the values of the solution ϕ is plotted as a function of T and ξ. The negative soliton is on the left at first, followed by the negative soliton on the right. We can see that negative kinks retain their shapes after collision, but this is more clear in figure 5.6, where we show different solutions as T increases.

Consider figure 5.6, where we show the solution for six different values of T. We plotted electrostatic potential ϕ versus the values of x, where the negative kink overtake a negative soliton. Initially, at $T = 0$ the negative kink is shifted 200 units to the left and then added to a negative soliton that is shifted 100. At $T = 400$, the kink caught up with the soliton. At $T = 500$, the collision solution is illustrated. As T is increased further, the soliton separates from the structure, and the original kink reappears moving at the same rate. Importantly, the soliton has the sharp drop rather than a rapid increase in ϕ which shows the solution at $T = 600$.

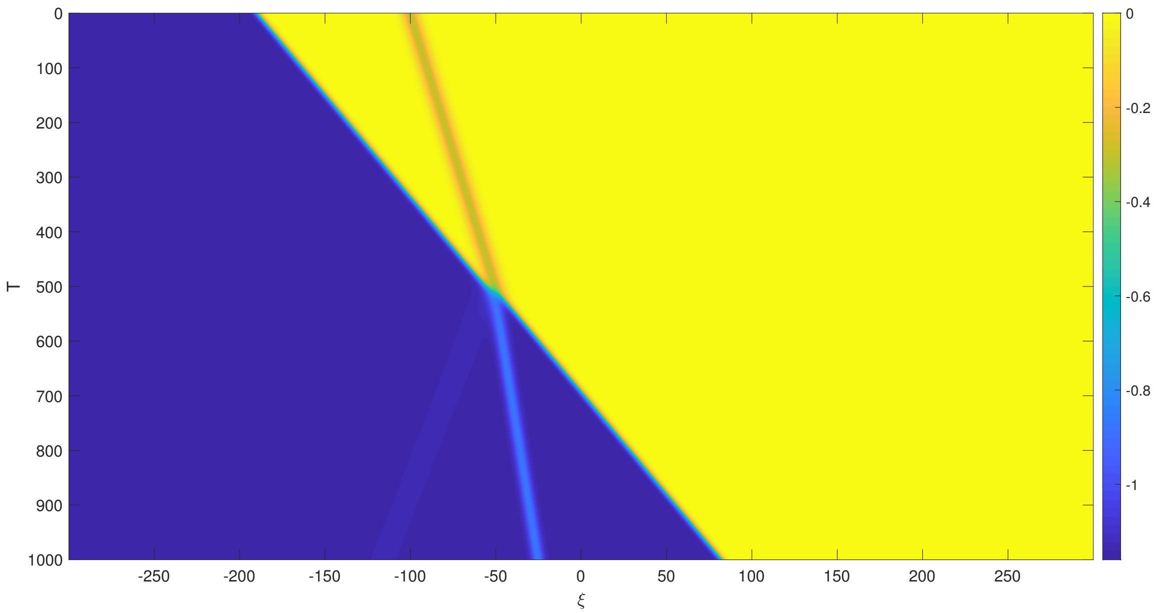

Figure 5.5: A kink overtaking a negative soliton. The electrostatic potential ϕ as a function of T and ξ is plotted.

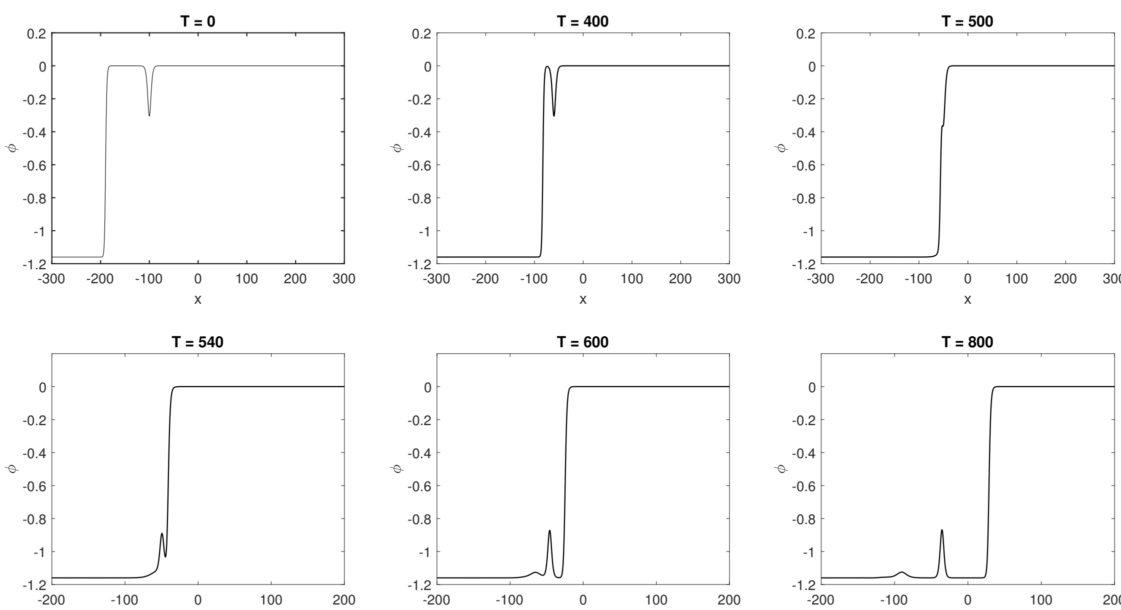

Figure 5.6: Snapshots of a kink overtaking a negative soliton.

Considering the findings of Olivier and Verheest [44], they conducted a simulation study of overtaking collisions between a positive soliton and a positive kink of a Gardner equation. After the collision, a kink re-emerges and the soliton has the opposite polarity, resulting in a dip rather than an increase in ϕ. Following the collision, the soliton and double layer propagate at the same rate as before. The results of our simulations are consistent with the observations made by Olivier and Verheest in 2020.

5.4 Collision between negative kink and positive soliton

Finally, we simulate a collision between a negative kink and a positive soliton. To simulate a collision, we combine these two initial conditions by shifting the soliton initial condition far away from the kink's center. The speed of the positive soliton is $m = 0.01$, and the speed of the negative soliton is $m = 0.10$, with $N = 6000$, $L = 600$, $k = 0.0001$ and $\theta = -0.10$. Figures 5.7 and 5.8 depict the resulting collision.

Consider figure 5.7, where the magnitude of the solution ϕ is plotted as a function of T and ξ. The negative soliton is on the left at first, followed by the negative soliton on the right. We can see that a negative kinks retain their shapes after collision, but this is clearer in figure 5.8, where we show different solutions as T increases.

Consider figure 5.8, where we show solutions for six different values of T. We plotted electrostatic potential ϕ versus function x, where the negative kink overtakes a positive soliton. At $T = 0$, the negative kink is shifted 200 units to the left of the center and then added to a positive soliton that is shifted 100 units. The kink caught up to the soliton at $T = 700$ marking the start of the collision. At $T = 900$, the collision is in full effect. When T is increased further, the original kink reappears. However, the soliton fails to form in the tail of the kink. Instead, a dispersive negative disturbance appears in the tail of the kink. This suggests that the soliton is destroyed during the collision. This result is in stark contrast to the collision bewteen a negative soliton and a negative kink, discussed in Section 5.3, where the soliton re-emerged with opposite polarity after the collision.

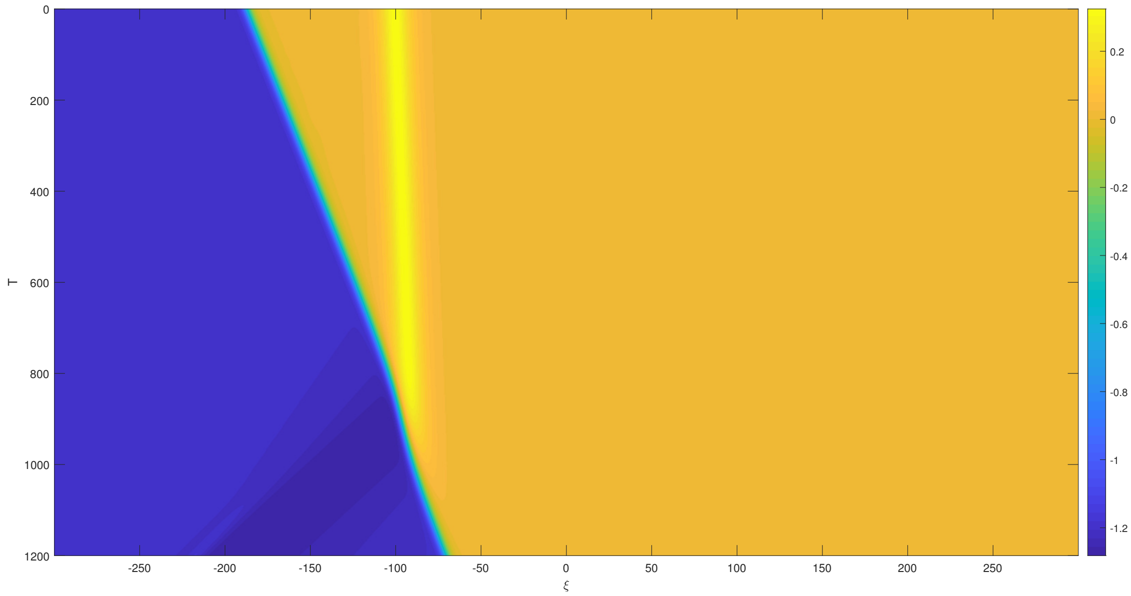

Figure 5.7: A negative kink overtaking a positive soliton. The electrostatic potential ϕ as a function of T and ξ is plotted.

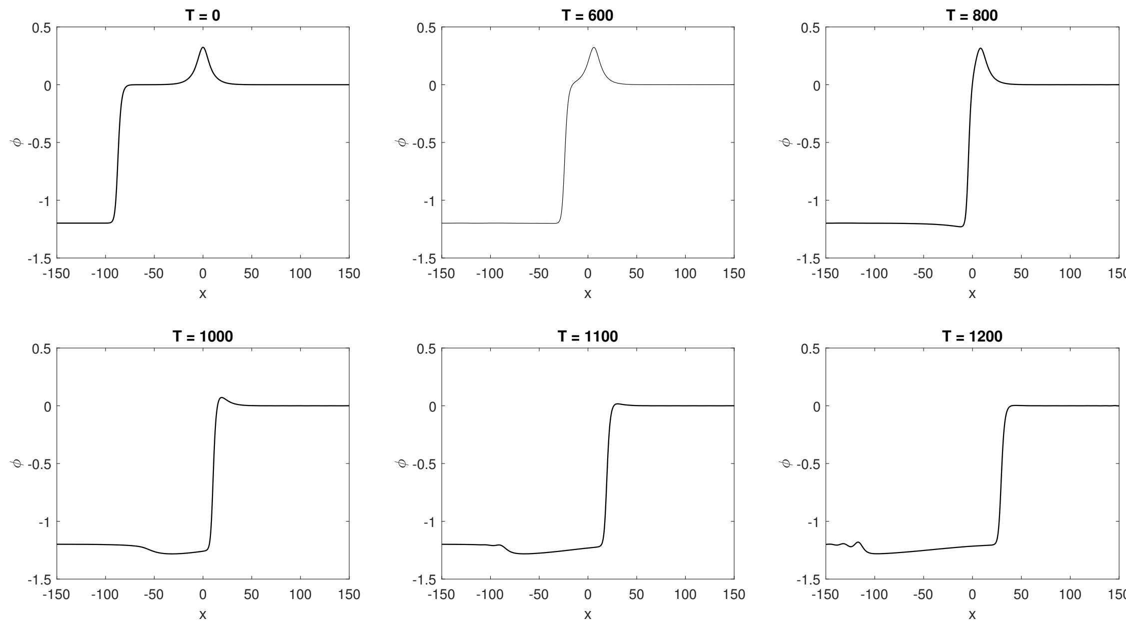

Figure 5.8: Snapshots of a negative kink overtaking a positive soliton. The time is indicated in at the top of each panel.

5.5 Summary of simulations

An mG equation was used to simulate the collision properties of nonlinear waves. We simulated solitons and kink solutions numerically. According to the numerical simulations, solitons retain their shapes after colliding with faster and slower solitons. When a positive and a negative soliton collide, the solitons retain their shapes after the collision. As a result, the collision is inelastic. To investigate collisions between kinks and solitons, a numerical simulation of the Gardner equation is used. In the first case, the results show that the kink is unaffected by the collision. However, the soliton that emerges from the collision has the polarity of the soliton that existed prior to the collision. In the second case, the results show that the kink remains unaffected after collision, but the soliton breaks up.

Chapter 6

Conclusion

The primary goal of this dissertation is to investigate solutions of the mG equation and to perform simulations of the collision properties of soliton-type solutions. The Sagdeev pseudopotential has been helpful in identifying nonlinear waves from which precise details about their parametric regions of existence can be deduced. We discovered that if the conditions are met, a diverse range of nonlinear waves may exist near supercritical plasma compositions. The findings indicate a fascinating connection between supercritical plasma compositions and nonlinear waves.

We performed the analytical analysis of the parameter space of the mG equation to find regions where specific nonlinear solutions occur. We applied a moving frame analysis in order to find the solutions of the mG equation. When all coefficients are nonzero, no closed-form solutions are available. The solutions are obtained by numerically solving a nonlinear ODE.

We normalized the mG equation by reducing the analysis to a single variable and expressed it in terms of a single parameter θ. By using the moving frame analysis, the problem was reduced to a second order ordinary differential equation that can be studied through the roots of an associated cubic polynomial. This analysis allows one to find regions in terms of θ where the nonlinear waves occur, as well as their propagation speeds.

A crucial component to simulate collisions between solitons and other nonlinear waves is to construct appropriate initial conditions. It should be noted that the solutions need to be constructed on a sufficiently large interval. The numerical integration is not accurate enough to provide such solutions because the resulting solutions are unstable. We therefore examined the asymptotic behaviour of the regular solitons, algebraic solitons, kinks and supersoliton solutions. A Taylor series expansion was used to derive asymptotic behavior using the Sagdeev method.

A numerical scheme was developed to simulate collisions between the different types of nonlinear waves. A finite difference approximation is used to approximate the spatial derivatives and the Runge-Kutta method is used to integrate with respect to time. We applied periodic boundary conditions to simulate collisions between regular solitons and algebraic solitons, and Neumann boundary conditions for simulations of collisions between solitons and kinks.

The important results are discussed briefly below. First, we performed numerical simulations of a faster positive and slower positive soliton. The outcomes demonstrate that the faster soliton passes the slower soliton and that it is unaffected (maintains its shape) even after collision. As a result, the collision is inelastic. We simulated collision between a positive and a negative soliton, after collision they maintain their shapes.

The most interesting results come from collisions of solitons and kinks. We simulated a negative kink solution and a negative soliton, as well as collisions between negative kink solution and positive solitons. The simulations between negative kink solution and negative soliton show that, following the collision, the kink retains its shape while moving at the same speed, whereas the soliton transforms into a soliton with opposite polarity. As a result, polarities of solitons behind a kink differ from those of solitons in front of the kink. A collision between a positive soliton and a negative kink solution was also simulated. The results show that a kink remains unaffected by collision, but the soliton disintegrates. A deeper analysis of this dynamic is beyond the scope of this thesis.

Bibliography

[1] N. J. Zabusky, M. D. Kruskal. *Interaction of solitons in a collisionless plasma and the recurrence of initial states*, Phys. Rev. Lett. 15, 240-243 (1965).

[2] J. S. Russel. *Report on waves*, Rep. 14th Meet. British. Assoc . Adv. Sci., York John Murray, London pp.311-390 (1844).

[3] J. Boussinesq. *Théorie de l'intumescence liquide, applelée onde solitaire ou de translation, se propageant dans un canal rectangulaire*, Comptes Rendus de l'Academie des Sciences 72: 755–759 (1871).

[4] L. Rayleigh. *On waves*, Philos. Mag, vol. 1, no. 5, pp. 257–279, (1876).

[5] J. McCowan. *On the solitary waves.* Phil. Mag. 32(5), 45-58 (1891).

[6] M. Remoissenet. *Waves called solitons*, Concepts and Experiments, 3rd edn. Springer, Berlin Heidelberg, (1999).

[7] S. P. Novikov, S. V. Manakov, L. P. Pitaevsky , V. E. Zakharov. *Theory of Solitons* (Consultants Bureau, New York) (Russian Edition, 1980, Nauka, Moscow) (1984).

[8] A. Kasman. *A brief history of solitons and the KdV equation*, Current Science 115(8):1486-1496 (2018).

[9] E. Fermi , J. R. Pasta , S. M. Ulam. *Studies of nonlinear problems*, Los Alamos Sci. Lab . Rep. LA-1940 (1955).

[10] J. J. Ford. *Equipartition of energy for nonlinear systems*, J. Math. Phys. 2,387-393 (1961).

[11] E. A. Jackson. *Nonlinear coupled oscillators. I . Perturbation theory: ergodic problems*, J. Math. Phys. 4, 551-558 (1963).

[12] J. K. Perring , T. H. R. Skyrme. *A model unified equation*, Nucl. Phys. 31, 550-555 (1962).

[13] C. S. Gardner, J. M. Greene, M. D. Kruskal, R. M. Miura. *Method for Solving the Korteweg–deVries Equation.* Physical Review Letters. 19 (19): 1095–1097 (1967).

[14] S. V. Singh, G. S. Lakhina, R. Bharuthram, S. Pillay. *Electrostatic solitary structures in presence of non-thermal electrons and a warm electron beam on the auroral field lines.* Physics of Plasmas 18(12) (2011).

[15] H. Washimi, T. Taniuti. *Propagation of ion acoustic solitary waves of small amplitude*, Phys. Rev. Lett. 17, 996 (1966).

[16] D. J. Korteweg, G. de Vries. *On the change of form of long waves advancing in a rectangular canal, and on a new type of long stationary waves*, Philosophical Magazine 39, 422–443 (1895).

[17] T. Taniuti, C-C. Wei. *Reductive perturbation method in nonlinear wave propagation* I J. Phys. Soc. Japan 24 941–6 (1968).

[18] R. Z. Sagdeev. *Cooperative Phenomena and Shock Waves in Collisionless Plasmas,* Reviews of Plasma Physics, 4, 23 (1966).

[19] B. B. Kadomtsev, V. I. Karpman. *Nonlinear waves.* Soviet physics. Usp. 14, 40 (1971).

[20] N. Nishikawa, P. K. Kaw. *Propagation of solitary ion acoustic waves in inhomogeneous plasmas.* Phys. Lett A 50, 455 (1975).

[21] P. G. Drazin and R. S. Johnson. *Solitons: An Introduction* (Cambridge University Press, Cambridge, UK, 1989).

[22] A. E. Dubinov , D. Yu. Kolotkov. *Ion-acoustic supersolitons in plasma,* Plasma Phys. Rep.38, 909 (2012).

[23] A. Das, A. Bandyopadhyay, K. P. Das. *Dust ion-acoustic solitary structures in non-thermal dusty plasma,* Plasma Phys. 78, 149 (2012).

[24] F. Verheest, M. A. Hellberg, I. Kourakis. *Electrostatic supersolitons in three-species plasmas* , Phys. Plasmas 20, 012302 (2013).

[25] M. A. Hellberg, T. K. Baluku, F. Verheest, I. Kourakis. *Dust-acoustic supersolitons in a three-species dusty plasma with kappa distributions*. Plasma Phys. 79, 1039 (2013).

[26] S. V. Steffy, S. S. Ghosh. *Phase portrait analysis of super solitary waves and flat top solutions*, Phys. Plasmas 25, 062302 (2018).

[27] F. Verheest, M. A. Hellberg , I. Kourakis. *Ion-acoustic supersolitons in plasmas with two-temperature electrons:Bolzmann & kappa distributions*, Phys. Plasmas 20, 082309 (2013).

[28] F. Verheest, M. A. Hellberg, I. Kourakis. *Dust-ion-acoustic supersolitons in a dusty plasmas with nonthermal electrons*, Phys. Rev. E 87, 043107 (2013).

[29] S. K. Maharaj, R. Bharuthram, S. V. Singh, G. S. Lakhina. *Existence domains of dust-acoustic solitons and supersolitons*, Phys. Plasmas 20, 083705 (2013).

[30] F. Verheest. *Electrostatic nonlinear supersolitons in dusty plasmas*, Plasma Phys. 80, 787 (2014).

[31] S. V. Singh, G. S. Lakhina. *Ion-acoustic supersolitons in the presence of non-thermal electrons*, Commun. Nonlinear Sci. Numer. Simulat. 23, 274 (2015).

[32] A. Paul, A. Bandyopadhyay. *Ion acoustic solitary structures in a collisionless unmagnetized plasma consisting of nonthermal electrons and isothermal positrons*, physics.plasm-ph. arXiv:1605.09464v1 (2016).

[33] C. P. Olivier, S. K. Maharaj, R. Bharuthram. *Ion-acoustic solitons, double layers and supersolitons in a plasma with two ion- and two electron species*, Phys. Plasmas 22, 082312 (2015).

[34] C. P. Olivier, F. Verheest, S. K. Maharaj. *Small-amplitude supersolitons near supercritical plasma compositions*, Phys. Plasmas 83, 905830403 (2017).

[35] F. Verheest, M. A. Hellberg. *Electrostatic supersolitons and double layers at the acoustic speed* Phys. Plasmas 22, 012301 (2015).

[36] F. Verheest, C. P. Olivier, W. A. Hereman. *Modified Korteweg-de Vries solitons at supercritical densities in two-electron temperature plasmas,* J. Plasma Phys. 82, 905820208 (2016).

[37] C. P. Olivier, F. Verheest, W. A. Hereman. *Collision properties of overtaking supersolitons with small amplitudes*, Phys. Plasmas 25, 032309 (2018).

[38] A. E. Dubinov , D. Yu. Kolotkov. *Interpretation of ion-acoustic solitons of unusual form in experiments in SF6-Ar plasma*, High Energy Chem. 46, 349 (2012).

[39] A. E. Dubinov , D. Yu. Kolotkov. *Ion-Acoustic Super Solitary Waves in Dusty Multispecies Plasmas*, IEEE Trans. Plasma Sci. 40, 1429 (2012).

[40] D. J. Struik. *A Source Book in Mathematics, 1200–1800.* Princeton University Press (1986).

[41] M. Abramowits, I.A. Stegun. *Handbook of Mathematical Functions with Formulas, Graphs, and Mathematical Tables*, Applied Mathematics Series. National Bureau of Standards (1965).

[42] I. Langmuir. *The interaction of electron and positive ion space charges in cathode sheaths*, Phys. Rev, 33, 954–989 (1929).

[43] C. P. Olivier, F. Verheest, S. K. Maharaj. *A small-amplitude study of solitons near critical plasma compositions.* J. Plasma Phys. 82, 905820605 (2016).

[44] C. P. Olivier, F. Verheest. *Overtaking collisions of double layers and solitons:Tripolar structures and dynamical polarity switches.* Phys. Plasmas 27, 062303 (2020).